

CONDITIONING NEW BEHAVIOURS IN *SALMONELLA*

CONDITIONING NEW BEHAVIOURS IN *SALMONELLA* USING PHYSICAL AND
NON-PHYSICAL LANDSCAPES

BY JANICE TAI, B.SC.

A Thesis Submitted to the School of Graduate Studies in Partial Fulfilment of the
Requirements for the Degree Master of Science

McMaster University © Copyright by Janice Tai, May 2022

McMaster University MASTER OF SCIENCE (2022) Hamilton, Ontario (Biochemistry and Biomedical Sciences)

TITLE: Conditioning new behaviours in *Salmonella* using physical and non-physical landscapes AUTHOR: Janice Tai, B.Sc. (McMaster University) SUPERVISOR: Dr. Alexander P. Hynes NUMBER OF PAGES: xiii, 86

LAY ABSTRACT

Bacteria that encounter predictable changes in their environment can acquire anticipatory gene regulation. This may be similar to Pavlovian conditioning, a type of associative learning that involves pairing two unrelated stimuli and anticipatory behavioural changes. Since conditioning has not been well explored in bacteria, we investigate whether *Salmonella* can learn new behaviours by pairing two unrelated carbon sources, citrate and maltose. We leveraged a motility plate assay to define a new natural history. By pairing stimuli across a physical landscape, we can select for bacteria that learn to use citrate to anticipate maltose. Time-series imaging shows evidence of variants capable of swimming faster through maltose and unique swimming behaviours through repeated passaging. Similar passaging of *Salmonella* in broth allowed us to compare anticipatory regulation across physical and non-physical landscapes. From this investigation, we hope to further understand the learning capacity of bacteria and how bacteria exploit memory to solve problems.

ABSTRACT

Bacteria frequently encounter changes in their environment and must adapt accordingly. When these changes are predictable, there is evidence of anticipatory gene regulation. For example, the model enteric pathogen *Salmonella* has a well-defined natural history, typically only encountering iron in the lumen of the gut. However, this bacterium responds to the presence of iron not by upregulating genes needed to thrive in the lumen, but rather the iron-deplete epithelium, the subsequent environment it encounters. This may be similar to Pavlovian conditioning, a type of associative learning that involves pairing two unrelated stimuli and anticipatory behavioural changes.

Since conditioning has not been well explored in bacteria, we are investigating whether *Salmonella* can learn new conditioned responses by pairing two unrelated carbon sources, citrate and maltose. We leveraged a prototype of the Microbial Evolution and Growth Arena (MEGA)-plate motility assay to define a new natural history. By pairing stimuli across a physical landscape, we can select for bacteria that learn to use citrate to anticipate maltose and can quickly deplete the second carbon source. Time-series imaging of bacteria as they swim across the plate shows evidence of emerging variants capable of swimming faster through maltose and unique swimming behaviours through repeated passaging. This approach selects for the fastest swimming bacteria, not necessarily bacteria that have acquired anticipatory regulation. As such, further genetic and transcriptional analysis of the variants are necessary. Similar passaging of *Salmonella* in broth allowed us to compare anticipatory regulation across a physical and non-physical landscape.

Learning to anticipate environmental changes will provide a bacterium with a selective advantage, allowing it to outcompete its conspecifics which are slower to respond. From this investigation, we hope to provide insight into the learning capacity of bacteria and further understand how bacteria exploit memory to problem-solve.

TABLE OF CONTENTS

LAY ABSTRACT	iii
ABSTRACT	iv
TABLE OF CONTENTS	vi
LIST OF FIGURES	ix
ACKNOWLEDGEMENTS	xi
LIST OF ABBREVIATIONS	xii
DECLARATION OF ACADEMIC ACHIEVEMENT	xiii
CHAPTER 1: INTRODUCTION	1
<i>1.1 Bacterial response strategies to environmental changes</i>	2
<i>1.2 Bacterial memory</i>	7
<i>1.3 Salmonella enterica</i> serovar Typhimurium	8
<i>1.3.1 Adaptive prediction in Salmonella</i>	9
<i>1.3.2 Motility in Salmonella</i>	10
<i>1.3.3 Selecting Salmonella for conditioning experiments</i>	12
CHAPTER 2: DESIGN, VALIDATION AND OPTIMIZATION OF THE MEGA- PLATE	13
<i>2.1 A MEGA-plate approach to adaptive prediction</i>	13
<i>2.2 Materials and Methods</i>	16
<i>2.2.1 Bacterial strains and growth conditions</i>	16
<i>2.2.2 P22 bacteriophage amplifications</i>	18
<i>2.2.3 Phage sensitivity spot test assay</i>	18

2.3.4 Streptomycin (STR)-gradient mini-MEGA-plate assay -----	19
2.3.5 MEGA-plate construction -----	20
2.3.6 MALDI-TOF analysis -----	21
2.3 Results: Optimizing the mini-MEGA-plate prototype -----	21
2.4 Handling challenges of upscaling from mini-MEGA- to MEGA-plate -----	25
2.5 Optimizing the MEGA-plate cleaning protocol -----	27
2.6 First MEGA-plate run - upscaling the STR partition gradient experiment-----	35
2.7 Optimizing the MEGA-plate imaging set-up -----	39
2.8 Optimizing the MEGA-plate experimental protocol -----	43
2.9 Final MEGA-plate protocol with annotations -----	46
2.10 Future directions: Refine the experimental protocol -----	50
CHAPTER 3: ANTICIPATORY REGULATION TRAINING WITH ALTERNATING CARBON SOURCES -----	53
3.1 Learning via physical and non-landscape exposure -----	53
3.2 Conditioning with citrate and maltose -----	54
3.3 Materials and Methods -----	56
3.3.1 Bacterial strains and growth conditions -----	56
3.3.2 Citrate-maltose training in broth -----	57
3.3.3 Citrate-maltose training on the mini-MEGA-plate -----	58

<i>3.4 Training on a physical landscape with the mini-MEGA-plate</i> -----	59
<i>3.5 Determining limiting concentration ranges of carbon sources</i> -----	65
<i>3.6 Training with a non-physical landscape in broth</i> -----	67
<i>3.7 Summary of training</i> -----	70
CHAPTER 4: CONCLUSIONS AND FUTURE DIRECTIONS -----	73
REFERENCES -----	75

LIST OF FIGURES

Figure 1: Bacterial response strategies to environmental changes. -----	4
Figure 2: MEGA-plate design schematic. -----	14
Figure 3: Time series imaging of the evolution of STR resistance on the mini-MEGA-plate prototype. -----	24
Figure 4: Mini-MEGA-plate and MEGA-plate size comparison. -----	25
Figure 5: Challenges with handling the full-size MEGA-plate. -----	26
Figure 6: Evaluating the effectiveness of MEGA-plate cleaning protocols. -----	30
Figure 7: Evaluating the severity of contamination of a media-only MEGA-plate. -----	31
Figure 8: Overnight MEGA-plate bleaching and drainage set-up. -----	33
Figure 9: Uneven solidification of swim agar during the upscaling process. -----	36
Figure 10: Time series imaging of the upscaled STR partition gradient experiment on the MEGA-plate. -----	38
Figure 11: MEGA-plate overhead camera imaging set-up. -----	39
Figure 12: Optimized LED light source for MEGA-plate time series imaging. -----	41
Figure 13: Effectiveness of India Ink negative staining to improve bacteria visualization on a MEGA-plate experiment. -----	42
Figure 14: Minimizing the effects of the second agar layer on STR diffusion. -----	44
Figure 15: Accumulation of liquid on the agar interferes with the MEGA-plate experiment. -----	46
Figure 16: Time series imaging of <i>S. Typhimurium</i> LT2 passages one and two through the citrate-maltose stimuli pairing on a mini-MEGA-plate. -----	61

Figure 17: Time series imaging of <i>S. Typhimurium</i> LT2 passage three through the citrate-maltose stimuli pairing using a mini-MEGA-plate. -----	63
Figure 18: Determining the concentration range of limiting glucose for an overnight culture of <i>S. Typhimurium</i> LT2. -----	66
Figure 19: Determining the concentration range of limiting maltose for an overnight culture of <i>S. Typhimurium</i> LT2. -----	67
Figure 20: <i>S. Typhimurium</i> LT2 growth curve in M9 media with limiting maltose during citrate-maltose broth passage. -----	69

ACKNOWLEDGEMENTS

I would like to start off by thanking my supervisor, Dr. Alexander P. Hynes, who has been a supportive and inspiring mentor throughout my 3.5 years with the lab. I am grateful for his constant feedback and encouragement which has helped me grow in confidence as a researcher and scientific communicator. I would also like to thank my committee members Dr. Michael Surette and Dr. Brian Coombes for their continued guidance and suggestions throughout my M.Sc., especially during my troubleshooting process.

I want to specially thank Bert Visheau who has been instrumental in the design and construction of the polycarbonate and autoclavable MEGA-plate. This project could not have progressed as far as it did without his initiative and participation. I would also like to thank Rob Thorton from Laird Plastics for his help with providing us timely information about materials and hand-delivering samples. Thank you to Jason Gilbert for helping us secure access to a warm room and demonstrating an interest in the project.

It has been an absolute pleasure working alongside all Hynes Lab members. From the day-to-day brainstorming to giving constructive feedback during my practice presentations to helping transport the MEGA-plate, the Hynes Lab members have been incredibly supportive. My graduate school experience would not have been as positive and rewarding without the team.

LIST OF ABBREVIATIONS

LB – Lysogeny broth

TSB – Tryptic soy broth

TSA – Tryptic soy agar

MEGA – Microbial evolution and growth arena

OD – Optical density

KAN - Kanamycin

STR – Streptomycin

MALDI-TOF – Matrix-assisted laser desorption/ionization-time of flight

UV – Ultraviolet

FOA - Fluoroorotic acid

BSC – Biosafety cabinet

PEI - Polyetherimide

MCP – Methyl-accepting chemotaxis protein

CRISPR – Clustered regularly interspaced short palindromic repeats

RPM – Revolutions per minute

DECLARATION OF ACADEMIC ACHIEVEMENT

I, Janice Tai, declare this thesis to be my own work. I am the sole author of this document. The research associated with this thesis was completed by myself, with help from Bert Visheau (Prototype Machine Workshop, who built the MEGA-plate).

CHAPTER 1: INTRODUCTION

When investigating a phenotype of interest such as antibiotic resistance or protein expression, researchers will often engineer and select for constitutive mutants: cells that continuously express a gene product (Miller and Mekalanos 1990). While constitutive mutants display a consistent phenotype during experiments and can increase population fitness in select conditions, these mutants are likely too costly to maintain in dynamic environments with fluctuating levels of nutrients, stressors and other stimuli. When selective pressure is absent, constitutively producing these unnecessary proteins takes away resources for other protein expression (Dekel and Alon 2005). As a result, gene regulation exists to allow bacteria to thrive in their environments without losing the capacity to adapt to new ones (Stoebel, Dean, and Dykhuizen 2008). Understandably, bacteria that can survive under specific conditions and adapt to environmental switches have a fitness advantage that will likely be selected for through evolution. By leveraging the adaptive ability of bacteria, there is an opportunity to move beyond creating constitutive, even inducible, mutants and instead generate populations of bacteria that can learn and unlearn associations based on repeated exposure to paired environmental conditions. Accordingly, it may be possible to reprogram populations of bacteria like the microbiome at the level of functionality instead of at the level of composition. Moreover, this investigation will allow us to further understand how bacteria evolve and exploit memory to solve problems.

1.1 Bacterial response strategies to environmental changes

Bacteria are capable of responding to unpredictable environmental shifts. The simplest strategy for responding to environmental changes is through direct sensing of a stimulus and mounting a related response (Fig. 1a). This is evident in the case of the *lac* operon where the presence or absence of lactose acts as a direct regulator of operon expression (Beckwith 1967). In the absence of lactose, the lacI repressor binds the operator and blocks transcription of the *lac* genes. When lactose is present, it binds and alters the repressor such that it can no longer interact with the operator and transcription can proceed. When shifts in the environment are unpredictable, bacteria may also undergo stochastic switching (Fig. 1b). Random shifting of cells to alternative cellular states appears to be a method of bacterial persistence that allows a portion of the population to be prepared for unexpected environmental changes (Acar, Mettetal, and van Oudenaarden 2008; Balaban et al. 2004). For example, when a genetically homogenous population of *Escherichia coli* was challenged with ampicillin, a portion of the surviving cells was characterized as ampicillin-sensitive with a reduced growth rate. The observed persistence was associated with stochastic phenotypic switching of cells between a normal and persister state (Balaban et al. 2004).

Bacteria that have well-defined natural histories often experience predictable environmental shifts and have a unique opportunity to acquire anticipatory regulation. If a preceding stimulus is a reliable indicator of a later stimulus, bacteria can leverage this temporal relationship and initiate a response to the later stimulus prior to actual stimulus exposure. Anticipation is advantageous because it takes time for bacteria to first sense,

then react accordingly to changes in their environment (Rolfe et al. 2012). If the upcoming environment is advantageous, for example nutrient-rich, bacteria that can anticipate the abundance of nutrients and activate the appropriate metabolic machinery will be able to consume the nutrients earlier and potentially faster. The remaining bacteria that simply react to the nutrients will reap less of this reward. On the other hand, if the upcoming environment is harmful, bacteria that have the ability to predict this stressor can mount the proper defense prior to encountering this danger and minimize the damage it incurs. In this case, bacteria that can anticipate a stressor will be protected earlier and better protected than bacteria that simply react to danger. For example, *E. coli* experiences a predictable increase in temperature and subsequent decrease in oxygen availability as the bacteria transition from the outside environment into the gastrointestinal tract. Tagkopoulos, Liu, and Tavazoie (2008) revealed that global transcriptional responses to elevated temperature and reduced oxygen levels were strongly correlated, suggesting that *E. coli* learned to associate the temperature-oxygen pairing. Specifically, a temperature increase resulted in transcriptional reprogramming from aerobic to anaerobic while in an aerobic environment, but in anticipation of an upcoming anaerobic niche. Conversely, transcriptional changes in response to oxygen depletion resulted in a heat shock response, mirroring an increased temperature environment. This anticipatory regulation has been selected for through evolution and allows cells to be more fit as they transition from the outside environment into the gastrointestinal tract. When a novel landscape was introduced (high temperature and high oxygen), the previous high temperature-low oxygen association was decoupled in fewer

than a hundred generations, suggesting that pairings of stimuli can be learned and unlearned (Tagkopoulos, Liu, and Tavazoie 2008). This form of anticipatory regulation, where either stimulus can induce both responses, is known as “symmetrical” (Fig. 1c).

In direct contrast, “asymmetrical” regulatory anticipation allows the preceding stimulus to activate both responses while the later stimulus can only activate its own response (Fig. 1d). This is akin to Pavlovian (classical) conditioning, the pairing of an unconditioned stimulus (S2) with a conditioned stimulus (S1) such that the S1 alone can elicit a conditioned response (R1). In Pavlov’s famous experiment (Pavlov 1927), the dog associated the sound of a bell (S1) with food (S2) and salivated (R1) in anticipation at the sound of the bell. This relationship is asymmetrical as the sound of a bell (S1) was not originally associated with food (S2) – by design, a ‘neutral’ stimulus. However, upon continued pairing of the food and bell, the previously neutral stimulus can now elicit a response associated with food. While research surrounding classical conditioning was originally intended for multicellular organisms, there is evidence that a similar learning paradigm, also referred to as adaptive prediction, exists in single-cell organisms (Fernando et al. 2009).

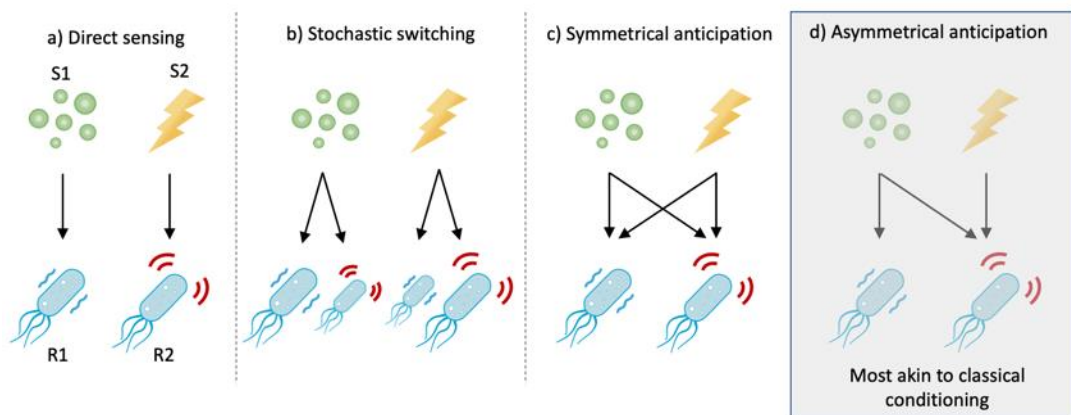


Figure 1: Bacterial response strategies to environmental changes. Bacteria rely on different response strategies when encountering unpredictable (a,b) and predictable (c,d) environmental changes. a) Under direct sensing, bacterium will elicit a unique response, R1 and R2, for each stimulus, S1 and S2 respectively. b) Under stochastic switching, cells will randomly shift to either R1 or R2 after sensing the stimulus. This appears to be a random process where a portion of cells enter an alternative state unrelated to the current environment. c) Under symmetrical anticipation, S1 and S2 can elicit both responses. d) Under asymmetrical anticipation, S1 can elicit both responses however S2 can only elicit its own response. This is most akin to Pavlovian conditioning. Adapted from Mitchell *et al.* (2009).

To define asymmetrical anticipation in a laboratory setting, Mitchell *et al.* (2009) generated three criteria: 1) to ensure unidirectionality of stimuli association, pre-exposure to S1 should generate a fitness advantage under S2 but not vice versa; 2) preparatory behaviour for S2 should be costly or neutral during S1 to ensure that this behaviour is conserved to reap a future reward that outweighs the preparatory costs; and 3) the association should be specific to S1 as opposed to other unrelated stimuli. This group investigated naturally occurring asymmetrical anticipation in *Saccharomyces cerevisiae*. In *S. cerevisiae*, the wine making process introduces predictable stresses where conditions are first highly acidic and osmotic, followed by a temperature increase and finally an eventual switch from fermentation to respiration (Mager and Hohmann 1997; Bauer and Pretorius 2000), which generates reactive oxidative species stressors (Maris et al. 2001). Pre-exposure to heat shock resulted in early preparatory behaviour for the anticipated

stressor, specifically induction of a cluster of genes related to oxidative stress. Additional examples of adaptive prediction can be observed in *Vibrio cholerae*, where late-stage infection predicts the subsequent aquatic environment and initiates expression of beneficial genes for post-shedding survival (Schild et al. 2007), and *Mycobacterium tuberculosis*, where hypoxia predicts subsequent re-aeration and aids in cell-cycle re-entry (Eoh et al. 2017). Adaptive prediction appears to be ubiquitous in single-cell organisms with temporally predictable niches.

While pre-existing adaptive prediction and *in silico* models of behavioural training have been relatively well explored (Tagkopoulos, Liu, and Tavazoie 2008; Fernando et al. 2009; Mitchell et al. 2009; Schild et al. 2007; Eoh et al. 2017), there is little literature investigating the ability of bacteria to learn conditioned behaviours by defining a new environment *in vitro*. Lopez *et al.* (2017) successfully created an association in *S. cerevisiae* between caffeine, a neutral stimulus that is linked to several regulatory and signaling pathways (Kuranda et al. 2006; Rallis, Codlin, and Bähler 2013) but does not inherently elicit responses related to the upcoming stressor, and a sublethal dose of 5-fluoroorotic acid (FOA), which is metabolized into a toxin by the URA3 enzyme. Survival assays revealed that within 50-150 generations, *S. cerevisiae* that were conditioned with caffeine prior to 5-FOA exposure had increased survival relative to bacteria without caffeine conditioning. This study also demonstrated that the adaptive mechanism responsible for this pairing involved numerous mutations leading to caffeine-initiated localization of URA3 to the peroxisome, which was absent in unconditioned cells (López García de Lomana et al. 2017). This is a promising study demonstrating that

novel environment structures can lead to adaptive prediction via coupling of unrelated response pathways.

1.2 Bacterial memory

For adaptive prediction to take place, there must also be memory to allow for pattern recognition and activation of the learned response. Without memory, the current environment has no given context or reference. Each stimulus will be interpreted as new and unique, regardless of whether or not it truly is. As such, having a memory of some sort is imperative for learning. In the *S. cerevisiae* example described above, the memory in question is encoded genetically through the accumulation of mutations (López García de Lomana et al. 2017). Beyond mutations, genetic memory can be actively acquired as demonstrated with Clustered Regularly Interspaced Short Palindromic Repeats (CRISPR). CRISPR consists of multiple repeat sequences that physically separate spacers, which are short DNA sequences acquired from interactions with foreign DNA such as injected phage genomes (Barrangou et al. 2007). Spacers are transcribed from CRISPR RNAs which are then complexed with specific Cas proteins. CRISPR RNAs act as a guide to target sequences that are complementary to the spacer sequences and the Cas protein functions as an endonuclease to cleave the targeted DNA and render it harmless (Mojica et al. 2009; Garneau et al. 2010). This acts as an adaptive immunity that allows bacteria to have a memory of and protection from previously encountered or similar phages.

This “memory” can also be transient, for instance when a past response results in lingering changes or properties that would take many generations before the “memory” is

lost (Lee et al. 2018). Hysteric or history-dependent responses are an example of bacterial memory, as demonstrated by the *lac* operon (Ozbudak et al. 2004). Depending on whether cells are preinduced or uninduced, exposure to low concentrations of TMG, a *lac* operon inducer, will result in differential operon expression. Preinduced cells have greater operon expression as they have high permease content, meaning even at lower concentrations of inducer, the intracellular inducer concentrations will be sufficiently high (Novick and Weiner 1957). In addition, daughter cells of induced cells will inherit the permeases and also induce at lower levels, resulting in a generational effect despite not being genetic (Novick and Weiner 1957). This suggests that later expression of the *lac* operon depends on a past event or memory, whether the cells were previously induced (Ozbudak et al. 2004; Novick and Weiner 1957). On a relatively shorter timescale, memory is also important for chemotaxis, a gradient-generated motility toward attractants like nutrients or away from repellents such as toxins (Macnab and Koshland 1972). Specifically, bacteria must have a brief memory of the previous concentrations of attractants or repellents in order to sense gradients. Without it, chemotaxis is not possible. Bacterial memory comes in many forms and is essential for learning.

1.3 *Salmonella enterica* serovar Typhimurium

Salmonella enterica serovar Typhimurium is a gram-negative, facultatively anaerobic bacterial pathogen that is a frequent cause of foodborne gastroenteritis (Majowicz et al. 2010). *S. Typhimurium* is one of several serovars that are host generalists, meaning they have broad host specificity (Gal-Mor, Boyle, and Grassl 2014).

The LT2 strain has been well characterized and is commonly used for molecular biology in *Salmonella* (McClelland et al. 2001).

1.3.1 Adaptive prediction in *Salmonella*

This enterobacterium has a well-defined natural history through the gastrointestinal tract and displays several instances of adaptive anticipatory behaviour (Baumbach et al. 2012; Altier 2005). *S. Typhimurium* preferentially infects epithelial microfold cells located at the Peyer's patch in the ileum (Jones, Ghori, and Falkow 1994). As a result, the bacterium can associate specific environmental cues with the upcoming presence of target host cells and mount an adaptive anticipatory invasion response. Prior incubation of *S. Typhimurium* in conditions characteristic of the small intestine, such as high osmolarity, low oxygen levels and the presence of bile, resulted in increased transcriptional activity of invasion-related virulence factors and invasion of cells compared to controls (Baumbach et al. 2012; Altier 2005). In addition, prior incubation of the bacterium in the presence of antimicrobial peptides, characteristic of a host immune response protecting against infection, repressed invasion (Baumbach et al. 2012). This suggests that predictive temporal niches can provide valuable information about the upcoming environments and lead to anticipatory responses.

Another well-studied anticipatory environmental signal involves iron-mediated virulence. In its natural history, *S. Typhimurium* typically only encounters iron in the lumen of the gut. However, this bacterium responds to the presence of iron not by upregulating genes needed to thrive in the lumen, but rather virulence genes required for the epithelium, the subsequent environment it encounters (Harvey et al. 2011; Bjarnason,

Southward, and Surette 2003). Furthermore, prior incubation of *S. Typhimurium* in increasing concentrations of iron resulted in stronger adhesion to epithelial cells and increased invasion (Kortman et al. 2012). This may be similar to Pavlovian conditioning where the luminal bacterium has learned to associate the presence of iron with a subsequent absence of iron at the epithelium, acting as a signal to upregulate virulence genes for upcoming cell invasion.

1.3.2 Motility in *Salmonella*

Salmonella navigates its environment through chemotaxis, a gradient-generated motility toward attractants and away from repellents (Macnab and Koshland 1972). Methyl-accepting chemotaxis proteins (MCPs) are sensor molecules that allow bacteria to sense nearby attractants and repellents and move accordingly. *Salmonella* has nine MCPs that bind a variety of stimuli including amino acids, sugars, ions and oxygen (Adler 1966; Webre, Wolanin, and Stock 2003; Kondoh, Ball, and Adler 1979; Edwards, Johnson, and Taylor 2006). Four of the MCPs (Tsr, Tar, Trg, Aer) have homologs found in *E. coli* while the remaining five are unique to *Salmonella* (Hoffmann et al. 2017). Tsr and Tar (also named CheM in *Salmonella*) are the most abundant MCPs and bind directly to serine and aspartate, respectively (Adler 1966; Webre, Wolanin, and Stock 2003). Tar can also sense maltose indirectly through the periplasmic maltose binding protein (Hazelbauer 1975). Trg can mediate a response to three D-sugars including glucose, galactose and ribose (Kondoh, Ball, and Adler 1979). Tsr and Aer are involved in aerotaxis to guide cells toward optimal oxygen concentrations for growth by proton motor force sensing and electron transport sensing, respectively (Edwards, Johnson, and Taylor 2006). As for

Salmonella-specific MCPs, Tap is responsible for sensing the chemoattractant citrate and chemorepellent phenol (Yamamoto and Imae 1993) while McpB and McpC mediate a repellent response to L-cystine (Lazova et al. 2012). The remaining two MCPs have no known function, likely because McpA lacks a transmembrane domain and Tip lacks a periplasmic sensor domain (Frye et al. 2006; Hoffmann et al. 2017).

MCPs are closely associated to the histidine protein kinase, CheA. When MCPs are bound by a ligand, CheA engages in increased autophosphorylation and increases the phosphorylation levels on the chemotaxis response regulator, CheY. CheY is released from CheA and binds a flagellar protein called FliM. Upon binding, FliM changes the flagellar rotation from counterclockwise to clockwise. The previously coordinated flagella are momentarily disrupted when one or more flagella begin rotating in the opposite direction. This results in a characteristic tumble, a randomized change of direction, which is then followed by another run, which is a more coordinated swim (Webre, Wolanin, and Stock 2003; Patteson et al. 2015). This tumble-run behaviour is characteristic in swimming motility.

Salmonella also engages in swarming motility, a coordinated movement of a group of cells that spread rapidly over a surface (Harshey and Matsuyama 1994).

Swarmer cells often differentiate when moist growth surfaces are present. These cells are elongated and hyperflagellated which allows them to move more quickly than a normal swimmer cells. In addition, swarmer cells are propelled by exclusively counterclockwise or clockwise rotation of the flagellar motor. Consequently, swarming typically moves in

one direction and does not follow a nutrient gradient like chemotaxis, but does require chemotaxis proteins like CheY (Mariconda, Wang, and Harshey 2006).

1.3.3 Selecting *Salmonella* for conditioning experiments

Seeing as *Salmonella* already displays natural anticipatory behaviours, it is an ideal bacterium to use in our investigation. The genome of *S. Typhimurium* will likely already have seemingly unrelated co-regulatory networks which can be used as a starting point for selecting signals. Moreover, motility in *S. Typhimurium* has been well characterized and is a fundamental component of the primary experimental design. Lastly, while this thesis project focuses on a single bacterium, our collaborators will attempt to train bacteria in increasingly complex communities such two-species pairings and gut-derived communities. *S. Typhimurium* can easily be included into a fixed community for further investigation.

CHAPTER 2: DESIGN, VALIDATION AND OPTIMIZATION OF THE MEGA-PLATE

2.1 A MEGA-plate approach to adaptive prediction

We are leveraging the Microbial Evolution and Growth Arena (MEGA) plate design from Baym *et al.* (2016) that was originally used to study the evolution of antibiotic resistance. To the best of my knowledge, this is a unique approach to investigate laboratory adaptive prediction. The MEGA-plate is a large 2 ft x 4 ft petri dish with built-in partitions to create a physical landscape consisting of different media conditions. To define a new natural history, the physical landscape will consist of multiple repetitions of two unrelated stimuli (Fig. 2). The arena can be organized such that the motile bacterium will always encounter the first stimulus prior to the second. The inoculum is grown in a medium without either stimulus, as an opportunity to select against constitutive mutants that may have evolved. There is also flexibility in this design to attempt co-administration of stimuli in addition to sequential exposure. Comparison of the mutants arising from co-administration and sequential exposure of stimuli can provide insight for optimizing training conditions as well as mechanistic information about potentially new co-regulated pathways.

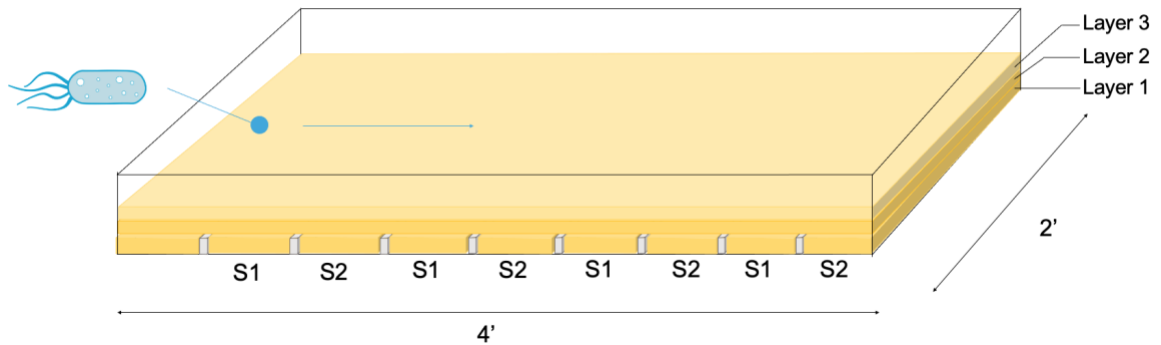


Figure 2: MEGA-plate design schematic. This large 2' x 4' petri dish has eight built-in partitions. “S1” denotes the first, neutral stimulus, “S2” denotes the second stimulus. The plate consists of two solid agar layers (layer 1 and 2) and one swim agar layer (layer 3). Bacteria are inoculated at one end of the plate and allowed to swim across the physical landscape undisturbed.

As illustrated in Figure 2, the MEGA-plate consists of three layers of agar. The first layer is a solid agar layer with the appropriate stimuli. The built-in partitions help minimize diffusion between media conditions. The second solid agar layer overlays the entire plate and functions to level off the first layer and prevent bacteria from interacting with the partitions. The third layer consists of a 0.28% swim agar overlaying the entire MEGA-plate. Motile bacteria are inoculated at one end of the plate with regular media and the plate is incubated at 37°C. Time series imaging is used to image the plate every 30 minutes from above. The MEGA-plate consists of nine equal partitions such that the length of exposure to each media condition is identical. However, there is flexibility to add additional temporary partitions to experiment with other parameters that may

influence conditioning such as stimuli exposure lengths and switch rates (Mitchell and Pilpel 2011; Boyer, Hérissant, and Sherlock 2021).

The MEGA-plate is a powerful method of investigation for the project for several reasons. First, by creating a new physical landscape, it takes advantage of *S. Typhimurium*'s motility and makes it relatively easy to visualize and separate the winners and losers. Winners, bacteria that have acquired anticipatory regulation, will be able to spread across the plate faster as they deplete nutrients in their vicinity and swim to access a reservoir of untouched nutrients (Berg and Brown 1972). Losers, bacteria that have not acquired beneficial anticipatory regulation, will be left behind. While adaptive laboratory evolution is commonly studied through serially passaging cultures in test tubes (Mitchell et al. 2009; Schild et al. 2007; Eoh et al. 2017; Adams and Rosenzweig 2014), even if mutants of interest arise, it will take many passages before those mutants start to dominate. Finding mutants of interest via culture passaging would therefore require much more time relative to the MEGA-plate approach. Secondly, time series imaging presents an opportunity to track variant lineages and follow evolution real-time. Since mutant lineages will compete for limited resources, it is likely that well adapted variants can exhaust nutrients locally and block growth of other less acclimated lineages (Berg and Brown 1972; Xavier and Foster 2007). Sampling variants of interest based on their location on the MEGA-plate will be relatively simple due to the physical separation of lineages as a result of fitness differences. Visual tracking, sampling and analysis of the variants will allow us to reconstruct the adaptation evolution that occurred. Lastly, the

large size of the plate allows us to simultaneously challenge large populations and increase mutational supply and diversification (Koirala et al., 2014).

On the other hand, the MEGA-plate approach presents some limitations. Due to the relatively long timeframe of this experiment, which is expected to be approximately a week based on previous optimizing runs, we are will likely be targeting genetic mutations that can be maintained through many generations. Other types of memory like hysteresis will eventually dilute out and may not be maintained after several generations. In the *lac* operon example, hysteresis of an induced state is lost after approximately 10-12 generations (Lambert and Kussell 2014). The duration of hysteresis will ultimately depend on protein stability, the initial number of proteins in the mother cell and the minimum number of proteins required to maintain the history-dependent phenotype (Lambert and Kussell 2014). Due to the relatively large distance between stimuli, cells may not experience both stimuli and must rely on robust generational memory in order to learn or recognize both stimuli. Lastly, variants will often be separated on the large propagating front. While this is beneficial for separating the winner from the loser, this distance reduces the chance of variants interacting to generate a fitter variant through horizontal gene transfer. As we experiment with training on the MEGA-plate, it will be important to keep these limitations in mind and find different approaches to address them.

2.2 Materials and Methods

2.2.1 Bacterial strains and growth conditions

Salmonella enterica serovar Typhimurium LT2 from The Félix d'Hérelle Reference Center for Bacterial Viruses (HER 1023) was purified through bacterial

streaking on 1% Tryptic soy agar (TSA) (Tryptone (Oxoid, Basingstoke, Hampshire, Cat. # LP0042B), Peptone from soybean enzymatic digest (Sigma-aldrich, Oakville, Canada, Cat. # 70178-100), D-glucose (Dextrose anhydrous, Fisher Chemical, Fair Lawn, USA, Cat. #D16-1), Sodium chloride (VWR Chemicals, Solon, USA, Cat. # BDH9286), Potassium Phosphate Monobasic (Fischer Chemicals, Fair Lawn, USA, Cat. #BP362500), Agar Molecular Genetics (Fisher BioReagents, Ottawa, Canada, Cat. # BP1423-500). A single bacterial colony was inoculated into 10 mL of TSB and incubated overnight with shaking at 130 RPM at 37°C. To create freezer stocks, 1.5 mL of culture was pelleted via centrifugation at 12000 RPM for 1.5 minutes. The pellet was resuspended in 800 µL of Tryptic soy broth (TSB) and 850 µL of resuspended bacteria was added to 150 µL glycerol (Fisher BioReagents, Fair Lawn, USA, Cat. # BP299-4) in screw-cap tubes. Freezer stocks are stored at -80°C.

S. Typhimurium SL1344 Δ SPI-1 and Δ *aroA* were obtained from the Coombes lab (McMaster University) and purified on 1% Lysogeny broth (LB) agar (Tryptone (Oxoid, Basingstoke, Hampshire, Cat. # LP0042B), Yeast Extract Molecular Genetics Powder (Fisher Scientific, Fair Lawn, USA, Cat. # BP1422-2), Sodium chloride (VWR Chemicals, Solon, USA, Cat. # BDH9286), Agar Molecular Genetics (Fisher BioReagents, Ottawa, Canada, Cat. # BP1423-500). These strains were stocked using LB media with the previously mentioned protocol. These attenuated strains were tested as potential strains of interest which would be safer to work with in large volumes on the MEGA-plate compared to *Salmonella enterica* serovar Typhimurium LT2. Ultimately, the attenuated strains were not used because of weaker P22 bacteriophage infectivity

relative to *S. Typhimurium* LT2, which we hope to incorporate via P22 transduction to accelerate evolution by reshuffling the genome.

S. Typhimurium was grown overnight in LB with shaking at 130 RPM at 37°C for all experiments performed within Chapter 2.

2.2.2 P22 bacteriophage amplifications

Salmonella enterica serovar Typhimurium LT2 temperate phage P22 was amplified from the Félix d'Hérelle Reference Center for Bacterial Viruses' collection (HER 161). For the primary amplification, 100 µL of overnight *S. Typhimurium* LT2 culture and a frozen scraping of P22 were mixed into 10 mL of TSB. The culture was incubated for 5 h with shaking at 130 RPM at 37°C and filtered through a 0.45 µm syringe filter (Fisher Scientific, Pittsburgh, USA, Cat. # 13-1001-07). The first amplification lysate was stored at 4°C. For the second amplification, 100 µL of overnight *S. Typhimurium* LT2 culture was added to fresh TSB and incubated with shaking at 130 RPM at 37°C until a mid-log OD of 0.3 was reached. A 50 µL inoculum of P22 first amplification was added to the mid-log culture and incubated for 4 h with shaking at 130 RPM at 37°C. The culture was filtered through a 0.45 µm syringe filter and stored at 4°C. Frozen stocks were also made by transferring 850 µL of P22 second amplification into screw-cap tubes with 150 µL of glycerol and stored at -80°C.

2.2.3 Phage sensitivity spot test assay

Spots tests are performed using a soft agar overlay method. 3 mL of 0.7% molten agar is aliquoted into separate soft agar test tubes and kept at 55°C in a heating block. 300 µL of overnight bacteria is added to the molten agar aliquot and spread on 1% LB agar

plates. When the soft agar has solidified, 3 μ L of undiluted bacteriophage lysate is spotted in the middle of the plates and allowed to dry. The plates are inverted and incubated overnight at 37°C.

2.2.4 Streptomycin (STR)-gradient mini-MEGA-plate assay

The mini-MEGA-plates were designed as a smaller prototype of the MEGA-plate using Nunc™ OmniTray™ Single-Well Plates (Thermo Fisher Scientific, Rochester, USA, Cat. # 242811). The plates are divided into 4 equal sections along the long edge of the plate, each section's area measuring 2.9 x 7.5 cm. These measurements are marked on the bottom of the plates and used as guides when using temporary partitions for pouring different media conditions. Disposable pipetting reservoirs (VWR International, West Chester, USA, Cat. # 89094-676) are cut to size (7.5 cm length) using ethanol-sterilized scissors, soaked in an ethanol bath for appropriate 20 minutes, and air dried in the Biosafety Cabinet (BSC). These reservoirs function as temporary partitions required for pouring sections of 1% LB solid agar containing increasing concentrations of STR (Streptomycin sulfate, Streptomyces sp., EMD Millipore Corporation, Burlington, USA, Cat. # 5711-100). For each section, 5 mL of 1% LB solid agar is aliquoted into a test tube and the appropriate amount of STR is added. The test tubes are vortexed gently and contents of the tubes are poured into the appropriate section of the OmniTray plate. Once the agar has set, the temporary partition is removed and placed at the next section's measurement marking. The same partition is used for all sections within one plate. A total of four different STR concentrations of LB agar are poured for a total of 20 mL composing the first layer. Approximately 25-30 mL of 0.28% LB swim agar is overlaid,

ensuring that the first layer of agar is completely covered. A 1 μ L inoculum of overnight bacterial culture is spotted 1 cm from the edge of the plate (equidistance from the top and bottom edge) on the section with no STR. The plates are secured with parafilm and incubated at 37°C in the Epson Perfection V850 Pro Scanner (Model J221B, Seiko Epson Corporation, Indonesia). A bash script is used to capture time series images every 30 minutes for the duration of the experiment through the Raspberry Pi 3 (B+ Model) (adapted from French, Coutts, and Brown 2018). The images are compiled in iMovie to create time series imaging.

2.2.5 MEGA-plate construction

The design of the MEGA-plate is largely based on the original Baym *et al.* (2016) paper. All construction of the MEGA-plate is performed by Bert Visheau at the Prototype Machine Shop in McMaster University's Health Sciences Centre. The MEGA-plate used for this project is made from polycarbonate and therefore is not autoclavable. The base of the plate is a 24 x 48 x 3/16 inch scratch-, UV-, and impact resistance polycarbonate sheet (McMaster-Carr, Robbinsville, USA, Cat. # 8707K125). The plate walls are 2 inches tall with a thickness of 1/2 inch and 3/8 inch for the long and short edges, respectively. The inner partitions are 1/2 inch tall and 1/8 inch in thickness. The polycarbonate used for the walls and partitions were provided by Bert. During the assembly of the plate, the polycarbonate was sanded to allow for solvent bonding using dichloromethane. A 24 x 48 x 1/4 inch clear, scratch-, and UV-resistant cast acrylic sheet (McMaster-Carr, Robbinsville, USA, Cat. # 8560K435) is used as the lid.

2.2.6 MALDI-TOF

MALDI-TOF analysis was performed under the guidance of Laura Rossi from the Surette Lab at McMaster University. Samples of interest were streaked to single colonies on 1% LB agar plates a day prior to the analysis. A single colony of each sample was transferred to the metal plate using autoclaved toothpicks, with special care taken to ensure each sample is contained within the outlined circular boundary. As a control, 1 μ L of a standard *E. coli* solution, provided by Laura, was also added onto the plate. Once the standard completely dried, 1 μ L of matrix, provided by Laura, was spotted on top of each sample and the control. When the samples were dried, the plate was analyzed using the Bruker MALDI Biotyper[®] (Identification Method: MALDI Biotyper MSP Identification Standard Method 1.1; Preprocessing Method: MALDI Biotyper Preprocessing Standard Method 1.1). Sample profiles were compared to the following Surette Lab inhouse libraries for identification: Main Spectra (MSP) Library(ies): Filamentous Fungi / contains 856 MSPs / cf603efb-38ec-41a3-b067-1973274b0870 / 2022-03-04T17:16:47.310, BDAL / contains 10833 MSPs / cb2dd1f0-1dc2-4fc0-83b7-83aa0eab5c76 / 2022-03-04T21:19:36.925, Mycobacteria Library (bead method) / contains 1069 MSPs / 29a7f7a4-c112-40b1-85fb-dea9f28b2a33 / 2022-03-04T16:35:38.003, Surette Lab / contains Surette Lab inhouse libraries.

2.3 Results: Optimizing the mini-MEGA-plate prototype

During the initial planning and building of the MEGA-plate, I experimented with a smaller prototype, a mini-MEGA-plate. Piloting this approach on a miniature version allowed me to test and optimize various experimental conditions in advance that I could

immediately implement when the MEGA-plate was complete. I used sterilized disposable pipetting reservoirs as temporary partitions to pour four different concentrations of streptomycin (STR)-agar slabs in a rectangular OmniTray (12.8 cm x 8.6 cm) plate. Next, I poured a layer of low percentage swim agar on top of the STR-agar and inoculated 1 μ L of overnight culture on the slab without STR. I used a flatbed scanner to image the plates every 30 minutes for 3-5 days and the images were compiled into a time series.

Several aspects of the mini-MEGA-plate experiment were optimized to create a standard protocol, including the following:

1) *Media*: *S. Typhimurium* growth and swimming were tested in both LB and Tryptic soy media. While there were no major concerns working with TSA, we opted to use LB media because the bacterium performs marginally better, and it is cheaper and easier to use.

2) *Swim agar*: Selecting an optimal swim agar concentration is important for the timeframe and result of the experiment. The agar concentration must be low enough such that *S. typhimurium* can swim freely with minimal obstruction. However, the agar concentration must also be high enough to solidify and maintain the stimulus gradient for the duration of the experiment. Three swim agar concentrations were initially tested. 0.35% swim agar resulted in highly inconsistent migration rates, often very slow or lack of swimming altogether. 0.25% and 0.3% swim agars produced more consistent swimming, with 0.25% agar resulting in more instances of faster swimming. However, there were a few occasions where the 0.25% swim agar, although solidified, would break or crack when the plates were moved. As a result, I tested 0.28% swim agar, similar to the original MEGA-

plate protocol (Baym et al. 2016), which resulted in consistent swimming and adequate rigidity such that the agar would not break (not shown).

3) *Incubation temperature*: I was interested to see whether our MEGA-plate experiments could be run at room temperature as this would be more convenient during the set-up and incubation process. Unfortunately, the migration rate for *S. Typhimurium* at room temperature was approximately 5x slower than at 37°C (ie. bacteria take 5 days vs 1 day of incubation to swim across a plate at room temperature and 37°C, respectively) and would not be realistic when running the experiment on a much larger plate. As such, plates will be incubated at 37°C for the duration of the experiment.

4) *Salmonella strain*: Since I would be working with relatively large volumes of culture on the MEGA-plate, I tested two attenuated strains which would be safer to work with as well as the virulent *Salmonella enterica* serovar Typhimurium LT2 strain. The attenuated strain *S. Typhimurium* SL1344 Δ SPI-1 lacks a portion of the type III secretion system involved in invasion, complex regulatory networks and virulence (Kröger et al. 2012; Lou et al. 2019). On the other hand, *S. Typhimurium* SL1344 Δ aroA lacks the ability to create its own aromatic amino acids (Bentley and Haslam 1990). Overnight growth in media across all three strains were similar, however *S. Typhimurium* LT2 swam more quickly and consistently than the attenuated strains. In addition, we hope to incorporate P22 bacteriophage transduction with the MEGA-plate experiments as a means to accelerate evolution by reshuffling the genome. P22 amplification on the attenuated strains were 1-log lower relative to *S. Typhimurium* LT2, suggesting weaker P22 bacteriophage infectivity. Moreover, the P22 plaque on *S. Typhimurium* SL1344 Δ SPI-1

and $\Delta aroA$ were much smaller and difficult to see. Black food colouring paste was used to stain the agar and attenuated bacterial strains in order to better visualize and count plaques, zones of bacterial clearing.

Ultimately, mini-MEGA-plate experiments using a 0.28% LB swim agar, inoculated with *S. Typhimurium* LT2, and incubated at 37°C provided the best results. I used these optimized parameters for the MEGA-plate upon its completion.

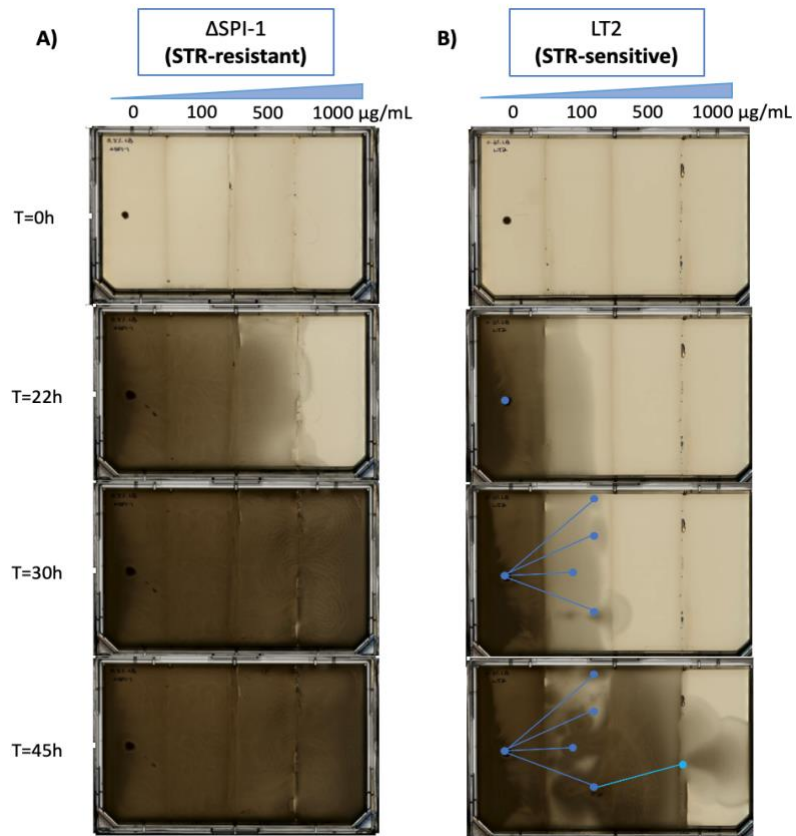


Figure 3: Time series imaging of the evolution of STR resistance on the mini-MEGA-plate. An increasing STR partition gradient (1, 100, 500, 1000 μg/mL) was used and

plates were inoculated with a) STR-resistant *S. Typhimurium* SL1344 Δ SPI-1, and b) STR-sensitive *S. Typhimurium* LT2.

Figure 3 depicts time series imaging of an optimization mini-MEGA-plate experiment at select timepoints. A STR concentration gradient of 0, 100, 500 and 1000 $\mu\text{g/mL}$ was used to observe the evolution of resistance in *Salmonella* when encountering increasing concentrations of STR. As expected, the plate inoculated with STR-resistant *S. Typhimurium* SL1344 Δ SPI-1 (Fig. 3a) did not show evidence of stalled swimming or mutation upon encountering various concentrations of STR. On the other hand, the plate inoculated with STR-sensitive *S. Typhimurium* LT2 (Fig. 3b) showed evidence of reduced motility (T=22 h, 30 h) or acquisition of STR-resistance (T=30 h, 45 h) at each antibiotic barrier. The blue nodes represent visual points of mutation or strain diversification while the blue lines represent tracking of variant lineages over time. This prototype demonstrates the strengths of using a MEGA-plate approach to investigate adaptive prediction including spatial separation of emerging variants and the ability to track and reconstruction any evolution that has occurred.

2.4 Handling challenges of upscaling from mini-MEGA- to MEGA-plate



Figure 4: Mini-MEGA-plate and MEGA-plate size comparison. The plate on the left depicts the OmniTray plates (12.8 cm x 8.6 cm) beside the MEGA-plate (2 ft x 4 ft).

Upon its completion, handling the MEGA-plate presented several additional challenges compared to the mini prototype. Figure 4 highlights the large size difference between the prototype and final product. First, moving the plate proved challenging. While the plate was well-built, the base is susceptible to bowing and the partitions can break off when the plate is twisted. In addition, the plate is heavy, especially when filled with media. To transport the plate safely and efficiently, I use a plywood board as a permanent supporting base and utility cart for moving (Fig. 5a). Secondly, the corners of the acrylic lid began to progressively warp creating gaps between the plate and lid. I suspect this is a result of temperature fluctuations during incubation in the warm room and used parafilm and bar clamps to seal the gaps (Fig. 5b). Lastly, it was important to determine a method for pouring media in a way that minimizes the risk of contamination. While the plate does not entirely fit into the BSC, pouring sections of the plate in the BSC and on the bench around flames were effective methods in reducing the risk of environmental contamination (Fig. 5c).



Figure 5: Challenges with handling the full-size MEGA-plate. These challenges include a) requiring a wooden base and utility cart to support and transport the plate, b) using bar clamps to seal gaps between the lid and plate due to warping of the lid, and c) pouring sections of agar in the BSC to minimize contamination.

2.5 Optimizing the MEGA-plate cleaning protocol

Since the MEGA-plate cannot be autoclaved, it is crucial to develop an effective protocol to sterilize and decontaminate the plate in between experiments. To create this protocol, I experimented with a single slab. To simulate an experimental run, I spread overnight cultures of *Salmonella* on a slab of 1% LB agar ensuring the bacteria contacts the plate edges and partitions. After an overnight incubation or until there was confluent growth, I proceeded with the cleaning protocol. To determine whether the cleaning protocol was adequate, I poured fresh 1% LB media into the cleaned section and checked for growth following an overnight incubation. I used the amount of growth as an indicator of whether additional sterilization steps were needed.

The initial cleaning protocol involved four sterilization steps. First, I soaked the bacteria and agar in 10% bleach for approximately one hour or until the bleach smell dissipated. I scooped out the bleached agar and bacteria as best as possible with double-gloved hands and used paper towels to remove the residual agar and bleach. Then, I sprayed and wiped the slab down with 70% ethanol followed by Power Quat, allowing the plate to dry in the BSC. Finally, while the plate was drying, it was exposed to UV light from the BSC for a minimum of 30 minutes. To evaluate the effectiveness of this protocol, I poured fresh LB media into the cleaned section. After an overnight incubation,

there was growth spreading from and spanning the partition and edges of the plate (Fig. 6a). Growths from different areas of the plate were sampled and tested against the *Salmonella*-specific P22 phage using a spot test. P22 phage formed plaques on the bacteria suggesting that the growths were likely a result of insufficient sterilization of the plate as opposed to environmentally introduced contaminants. Consequently, additional sterilization steps focusing on the partitions and edges were needed. In addition to the growths, I noticed bubble-like specks in the agar, however they were only seen at one end of the slab.

The cleaning protocol was modified to focus on sterilizing the edges of the plate and partitions. After the bacteria and agar were removed. I soaked the slab overnight in 10% bleach and removed the Power Quat step. This additional bleaching step greatly reduced the amount of growth seen when fresh media was added to the cleaned slab. There was notably less growth along the partitions and only two single colony growths (Fig. 6b), which were sampled and determined to be bacteria other than *Salmonella*. Three additional single colonies were seen in the following days and were likely contaminants introduced from the environment. The bubble-like specks previously seen were also present in the agar (Fig. 6b).

During my third attempt to sterilize the plate, I focused on determining the cause of the bubble-like specks. During a discussion with Dr. Baym regarding their plate cleaning protocol, he suggested that trying to remove all the bleach would risk introducing more sources of contamination, however I suspected the residual bleach was affecting the media and creating these specks. I followed the modified protocol

(bleaching agar, soaking the plate overnight in bleach, wiping with ethanol and disinfecting with UV light), this time ensuring that the plate was completely dry before pouring media. When I allowed all the liquid to evaporate, I did not see specks in the agar. In addition, there was no growth on the fresh media indicating that this modified protocol was sufficient for sterilizing the plate (Fig. 6c).

During my fourth attempt to standardize the MEGA-plate cleaning protocol, I focused on simplifying the steps. While filling and soaking one slab in 10% bleach was effective for sterilization, it might not be the most realistic solution for cleaning the entire plate with a total of 15 L of agar. As a result, I tested an alternative that involved spraying and wiping down the plate with a higher concentration of bleach (100%) twice. Only two single colonies of growth were seen on the fresh media (Fig. 6d), neither of which were *Salmonella*, suggesting they were environmental contaminants. I also noticed a droplet of water on the agar, likely condensation that fell from the lid. I was curious whether the underside of the lid required sterilization to prevent contamination from condensation droplets. I sampled the droplet which did not grow in LB broth, suggesting that the underside of the lid likely does not require separate sterilization. I left the plate at room temperature over the next several days and noticed an accumulation of condensation on the plate lid, some of which had fallen back onto the agar and plate. I also saw two new single colony growths that were not visible before and suspected they were growth from droplets of condensation or slow-growing bacteria. In future experiments, I planned to take an additional step to clean the underside of the lid using ethanol in case of

condensation. Overall, wiping the plate with 100% bleach was effective and a good substitute for soaking the plate in 10% bleach.

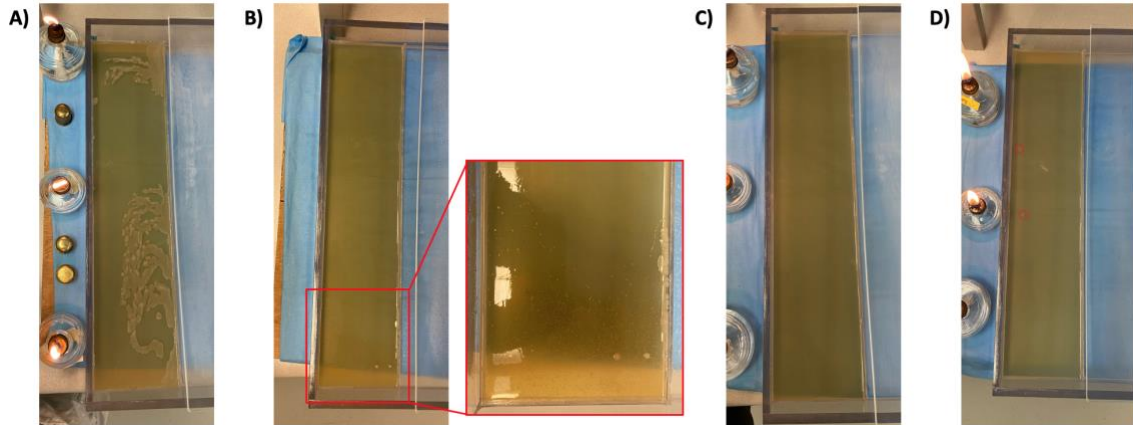


Figure 6: Evaluating the effectiveness of MEGA-plate cleaning protocols. To determine the effectiveness of various cleaning protocols, fresh LB media was poured into the slab post cleaning. The amount of growth after an overnight incubation was used to evaluate whether additional sterilizations steps were needed. A) Variation 1 of the cleaning protocol involved bleaching and removing the bacteria and agar, wiping with ethanol, spraying with Power Quat and drying under UV light. B) Variation 2 removes the Power Quat step and adds an additional overnight bleaching step. The zoomed-in section highlights the bubble-like specks seen in the agar and growth along the partition. C) Variation 3 makes a note of ensuring the plate is completely dry of bleach and ethanol before pouring in fresh LB media. D) Variation 4 replaces the overnight bleaching step with spraying the plate with higher concentrations of bleach. The red circles highlight two single colonies of growth.

When applied to the whole plate however, the aforementioned cleaning protocol was insufficient. Subsequent uses of the MEGA-plate revealed considerable amounts of

growth originating from the edges of the plate that could not be traced back to the inoculum. To understand the severity of the contamination, I conducted several MEGA-plate experiments containing only LB media, without an inoculum (Fig. 7). As a result, any growth seen on the plate can be attributed to contamination or insufficient sterilization between experiments. Using the previously designed cleaning protocol (bleaching agar, wiping with 100% bleach followed by 70% ethanol, and disinfecting with UV light), there was a large amount of growth along the edges of the plate and throughout the media (Fig. 7a).

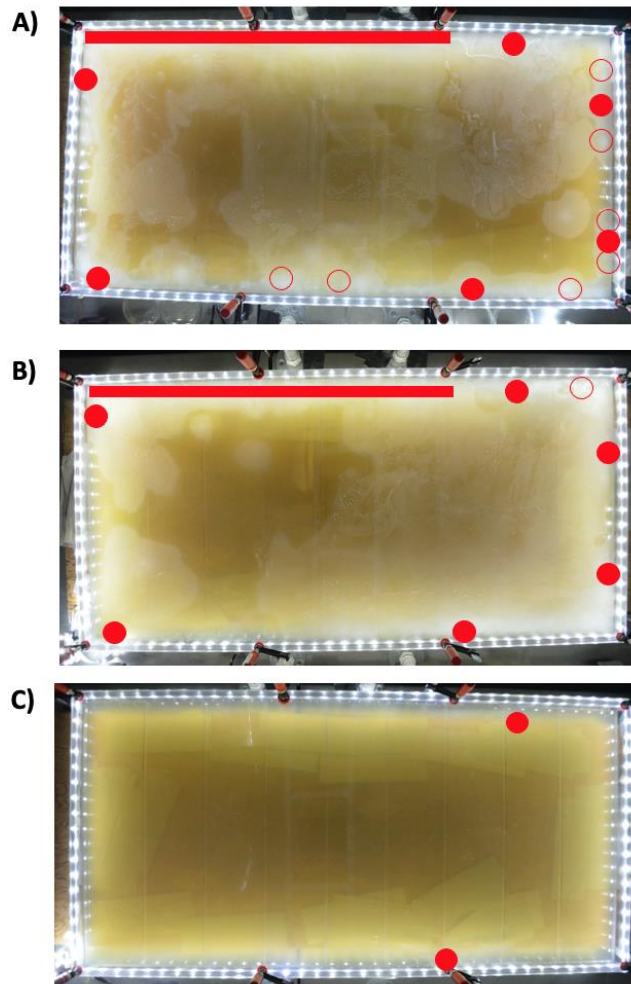


Figure 7: Evaluating the severity of contamination of a media-only MEGA-plate. Several cleaning protocols were tested for their effectiveness on the full-size MEGA-plate, including a) the previously designed cleaning protocol (bleaching agar, wiping with 100% bleach followed by 70% ethanol, and disinfecting with UV light), b) a modified protocol that substitutes wiping with bleach with overnight bleaching, and c) the most recent iteration that includes both overnight bleaching of the plate and the use of background kanamycin in the agar. The red circles and bars represent origins of growth along the plate edges identified through time series imaging. Filled circles and bars represent growths with the same origin on the plate across two or more media-only MEGA-plate runs. Empty shapes represent origins of growths that were only seen on one of the three cleaning protocols.

In an attempt to reduce contamination, I substituted the step for wiping down the plate with 100% bleach with overnight bleaching at 10%. I was originally hesitant to perform overnight bleaching due to the large amount of bleach that would be necessary to fill the plate, however it was evident that wiping with bleach was insufficient. After the bleached bacteria and agar were removed, I filled the plate with approximately 18 L of 10% bleach. By filling the plate with more bleach than the 15 L of media used in a MEGA-plate experiment, I can ensure that the walls of the plate that may have residual bacteria are submerged in bleach. To remove the bleach, I attached a serological pipette to one end of a plastic tubing and placed the other end in the bleach. The serological pipette was able to pull the bleach through the tubing and create enough of a pressure difference for the bleach to flow freely into a bucket (Fig. 8). I used a new serological pipette to

remove the residual bleach and allowed the plate to air dry in the BSC. With the addition of overnight bleaching, the number of growths along the edges of the plate were reduced but the contaminants continued to spread rapidly across the media (Fig. 7b).



Figure 8: Overnight MEGA-plate bleaching and drainage set-up. The bleach drainage set-up consists of using a serological pipette and plastic tubing to create a pressure difference that allows bleach to drain in a bucket.

I was interested in using background antibiotics to further suppress contamination. I identified 18 origins of growth on the MEGA-plate post overnight bleaching and tested these bacteria against different antibiotics. Kanamycin was selected as the background antibiotic because all the contaminants are kanamycin-sensitive while my bacterium of interest, *S. Typhimurium* LT2, is resistant. These contaminants were also tested against a *Salmonella*-specific phage, P22, and no plaques were seen. This suggests that the contaminants are not a result of insufficient sterilization of my bacterial inoculum. Using

the modified cleaning protocol with overnight bleaching in addition to background kanamycin resulted in a noticeable reduction of contamination, with only two points of growth (Fig. 7c). These growths were localized and spread more slowly compared to what was previously seen in Figures 7a and 7b. Several areas of growth were sampled, and matrix-assisted laser desorption/ionization-time of flight (MALDI-TOF) analysis identified the contaminants as *Staphylococcus hominis*, *Staphylococcus haemolyticus*, and *Victivallis vadensis*. I was surprised to see *V. vadensis* identified as one of the contaminants since this bacterium is strictly anaerobic, and my plates were grown in aerobic conditions (Zoetendal et al., 2003). Further investigation of these growths by streaking single colonies on a mannitol salt agar (MSA) plate, selective for *Staphylococcus*, suggests that the *V. vadensis* predicted by MALDI-TOF analysis is likely *Staphylococcus*. We also received confirmation that there was an error with the *V. vadensis* MALDI-TOF profile, further validating the identity of the growths. While *Staphylococcus* is characterized as non-motile, the growths appeared to have travelled across the agar. It is likely that the bacteria were able to spread through cracks in the agar that may have contained some liquid, which could help carry the bacteria. The most recent iteration of the cleaning protocol that has been tested for its effectiveness with LB media-only runs (bleaching agar, overnight bleaching, wiping with ethanol, and disinfecting under UV light) along with background kanamycin were implemented for all future MEGA-plate experiments.

In an attempt to replace the overnight bleaching step, which although effective is time-consuming and laborious, I experimented with the effectiveness of Power Quat

(Sani-Marc Inc., Victoriaville, Canada, Cat. #09-10073), a disinfectant that kills bacteria, viruses, mildew and yeast. I used a dilution ratio of 5.5 mL Power Quat / L of solution as indicated for use. Instead of overnight bleaching, I sprayed down the walls and base of the plate with Power Quat, and use Kim wipes to clean the surfaces twice. It is important to note that the instructions for disinfection state that surfaces should remain wet for approximately 10 minutes before excess fluid is removed. When analyzing time series imaging of the STR-gradient MEGA-plate experiment, which I performed after using Power Quat in the cleaning protocol, it appears that all growths can be tracked back to the original inoculum. To verify whether Power Quat can replace the overnight bleaching step, it will be important to do a LB media-only MEGA-plate run to look for contamination.

2.6 First MEGA-plate run - upscaling the STR partition gradient experiment

The purpose of the initial MEGA-plate runs is to determine whether I can successfully upscale my experiments from the mini- to full-size plate. For the first run, I attempted to upscale the STR partition gradient experiment, using increasing concentrations of antibiotic moving toward the middle of the plate (0, 100, 200, 500 and 1000 $\mu\text{g/mL}$). Different inoculum sizes of overnight *S. Typhimurium* LT2 were tested on the rightmost (20 μL) and leftmost (40 μL) slabs. Testing different inoculum sizes could provide insight into differences in migration rate and inform a standardized inoculum size for future experiments. The MEGA-plate was incubated in the warm room and the imaging set-up was adjusted accordingly to capture images every 30 minutes over 135 hours.

I faced several challenges further throughout the upscaling process. Firstly, during the pouring of the plate, I noticed that the swim agar had difficulty solidifying. While the swim agar along the edges of the plate appeared to have solidified, the middle portion was not set. The swim agar ripped in several areas and portions detached from the edges causing the agar to fold or ripple when the plate was transported to the warm room (Fig. 9). Since the swim agar had not completely set, movements during transportation likely agitated the agar and resulted in its breaking. Secondly, despite using light diffusers to reduce the glare on the plate from the overhead lights, the glare still interfered with imaging. Lastly, imaging was also hindered by the plate drying out. After 2 days of incubation, I noticed gaps between the lid and plate along the lengths of the plate which likely accelerated the drying.

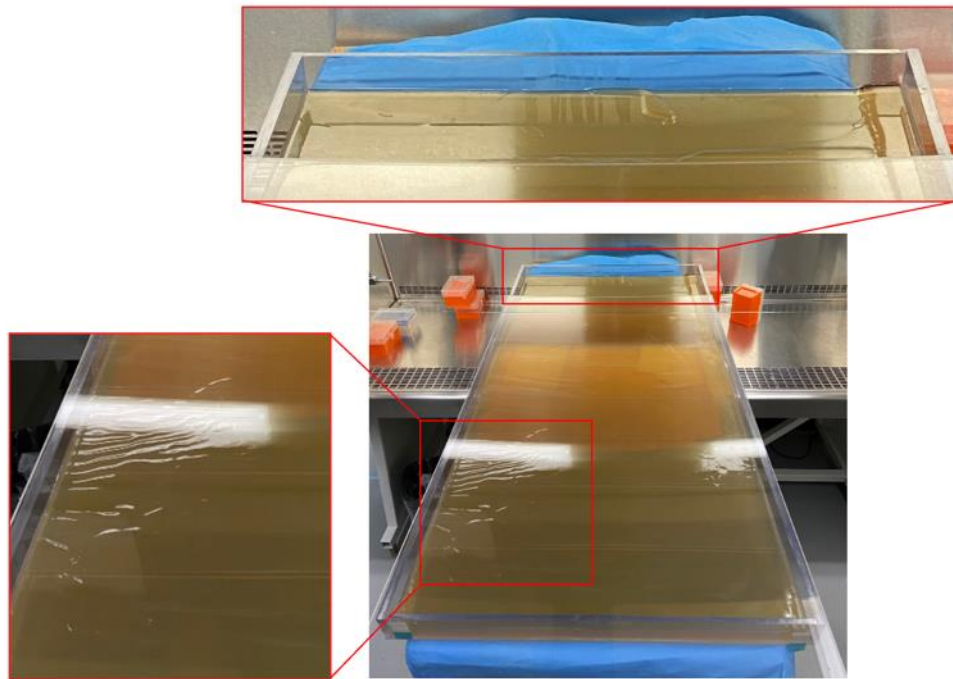


Figure 9: Uneven solidification of swim agar during the upscaling process. The top red box highlights an area of swim agar that detached from the edges of the plate. The red box on the left highlights the folding and rippling of the swim agar due to rips and unsolidified agar.

Figure 10 depicts time series imaging of the upscaled STR partition gradient experiment on the MEGA-plate. The plate was inoculated with STR-sensitive *S. Typhimurium* LT2 at both ends of the plate without antibiotics and imaged every 30 minutes over 135 hours. Despite interference from the glare and drying of the plate, the imaging captured evidence of STR-resistance acquisition at the 100 $\mu\text{g/mL}$ STR barrier, highlighted at T=51 h. This is similar to the phenotype seen on the mini-MEGA-plate (Fig. 3b). At T=60 h, it is evident that the plate is drying out and the drying appears to start from the middle. Over the course of the time series, the glare on the lid becomes progressively larger and is likely a result of the lid warping.

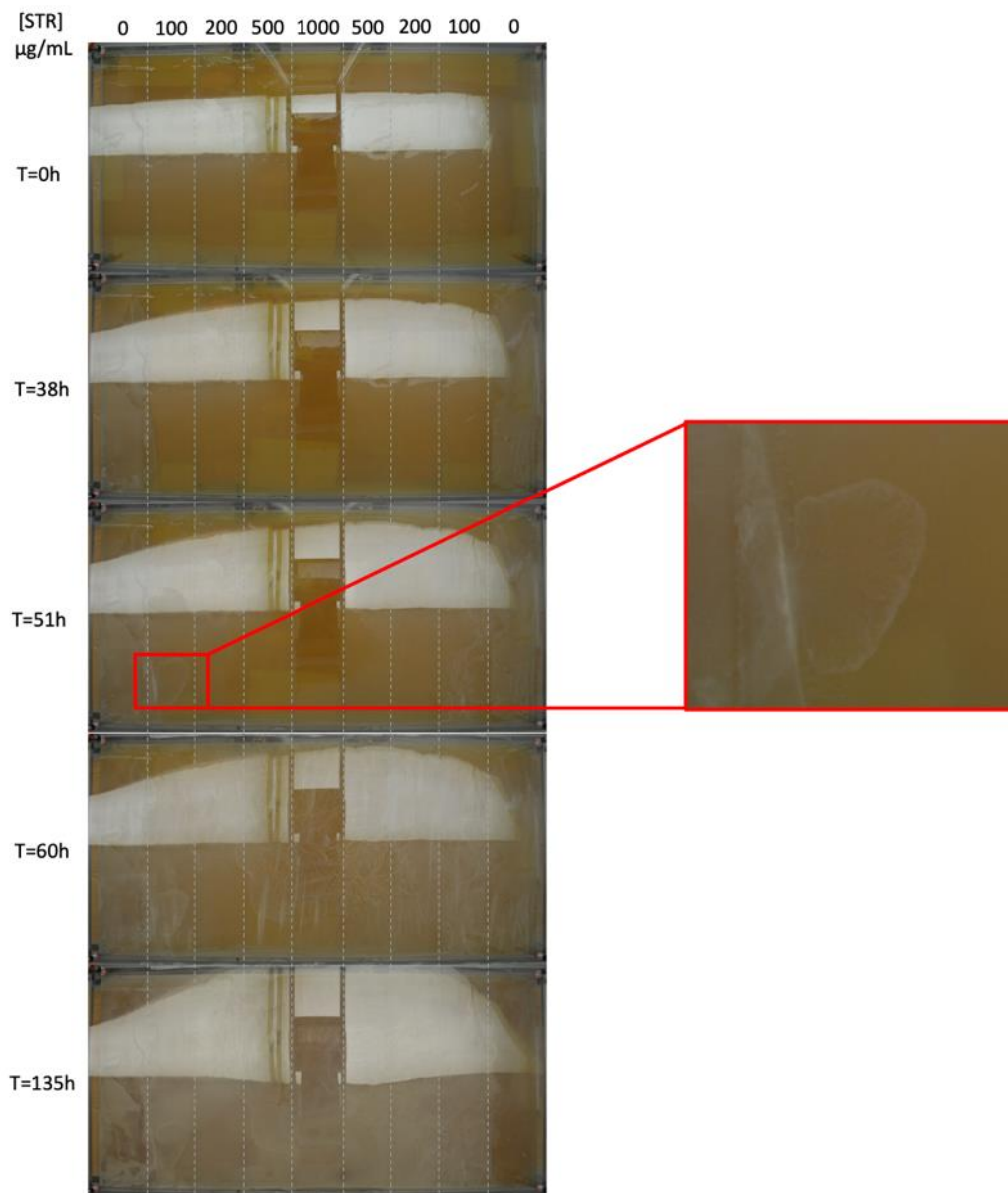


Figure 10: Time series imaging of the upscaled STR partition gradient experiment on the MEGA-plate. An increasing STR partition gradient (0, 100, 200, 500, 1000 $\mu\text{g/mL}$) was used in the experiment and images at specific time points are highlighted. The red box at T=51 h highlights the acquisition of STR-resistance in a *Salmonella* variant at the 100

$\mu\text{g/mL}$ STR barrier. The glare caused by the overhead lights increasingly interferes with imaging of the top half of the plate.

2.7 Optimizing the MEGA-plate imaging set-up

I built an overhead camera stand to capture time series imaging of the MEGA-plate. The stand resembles a table with a small platform at the top. The legs and overall structure of the stand are made from PVC pipes and fittings, and measured to ensure the entire MEGA-plate is captured. The legs are connected to flanges which can be taped to the table for stability (Fig. 11a). The platform holds the DSLR camera and consists of the following: 1) a Styrofoam box with a hole at the bottom to accommodate the camera lens; 2) two wooden boards screwed into the top PVC pipes to provide additional support for the camera; and 3) four wooden blocks taped to the boards and surrounding the Styrofoam box to prevent the camera from shifting during the time series (Fig. 11b). A Nikon D5200 is used to capture time series imaging using the built-in intervalometer function.

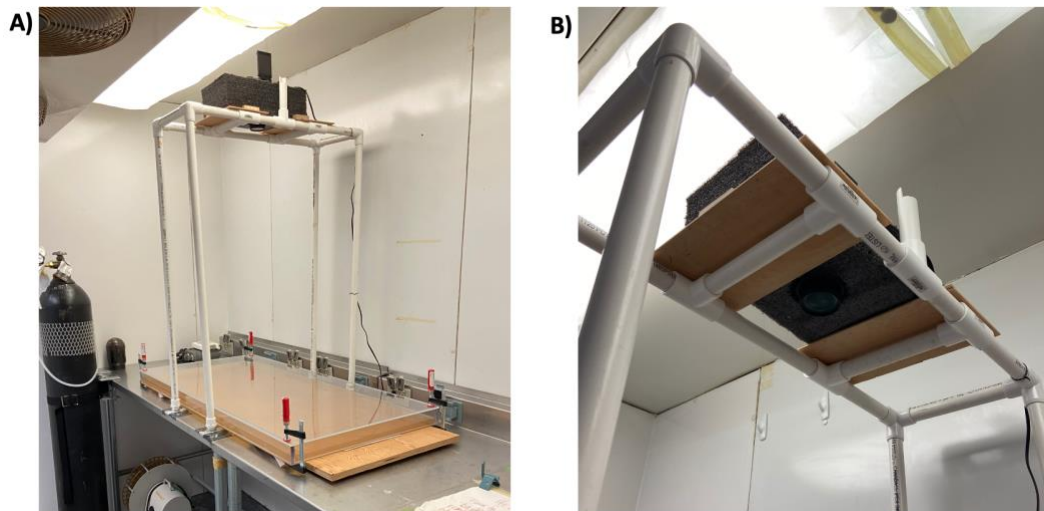


Figure 11: MEGA-plate overhead camera imaging set-up. The overhead camera stand used to capture time series imaging of the MEGA-plate consists of a) a table-like structure built from PVC pipes, fittings and flanges, and b) a platform to support the camera.

While the overhead camera stand adequately records time series imaging, several factors from the first run were identified as hindering the image quality. Most prominently, the overhead lights in the warm room produced a large glare that interfered with imaging. For subsequent experiments, I used an LED strip attached to the outer walls of the MEGA-plate as a light source and turned off the overhead lights (Fig. 12a). By increasing the ISO sensitivity of the camera to capture more light, I was able to eliminate the glare while capturing high quality images (Fig. 12b). To prevent the plate from drying out during incubation, I parafilmmed the sides of the plate and used bar clamps to seal gaps between the lid and walls of the plate. Lastly, to address previous challenges with the swim agar, it was crucial for each bottle of agar to have a magnetic stir bar. This allowed the agar cool down enough for the addition of antibiotics without solidifying. I also ensured the agar was completely melted prior to pouring and completely solidified before transporting the plate to the warm room. This resulted in a smooth top layer of agar that would allow bacteria to swim without restriction from ripples and breaks in agar. These modifications to the experimental and imaging set-up were implemented for all subsequent MEGA-plate experiments.

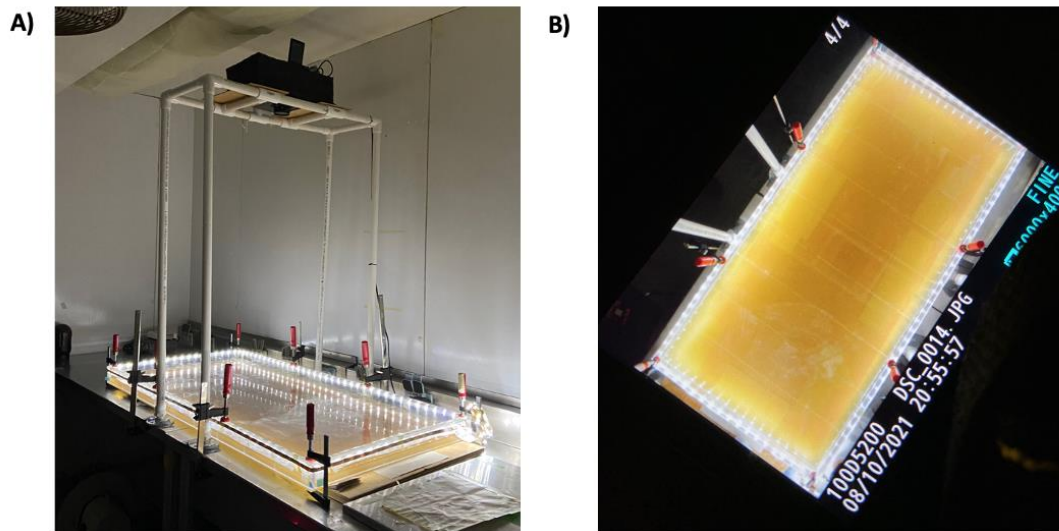


Figure 12: Optimized LED light source for MEGA-plate time series imaging. A) New imaging set-up using an LED strip taped to the outside of the plate. B) High ISO sensitivity enables high quality imaging.

To further improve tracking of bacterial movement through time series imaging, it is important to maximize the contrast between the bacteria and background agar. Although previous experimentation with negative staining on the mini-MEGA-plates made it more difficult to visualize bacterial motility, using a larger inoculum size and adjusting camera settings to maximize contrast may improve visualization. The negative charge of the bacterial membrane will repel the black India Ink so while the agar is coloured black, the bacteria will appear light or white-beige in colour. Camera settings were set to the following to optimize image quality: Active D-lighting = High; Auto ISO sensitivity = Off; ISO sensitivity = 1000. Figure 13 compares the image quality of a previous MEGA-plate experiment (Fig. 13a) to the most recent run that incorporates the mentioned adjustments (Fig. 13b). Negative staining effectively improved bacterial

visualization, resulting in light coloured bacteria against a dark background. Contrast was further enhanced with image editing on Preview to increase exposure and decrease shadow, saturation and sepia (Fig. 13b). While the India Ink improves bacteria visibility, there are foggy, white streaks concentrated at the left and right ends of the lid which greatly hinder the image quality. This haze is likely a result from cleaning the lid with ethanol and may not have been as visible when the background agar was yellow. The combinatory effects of negative staining and optimized camera settings helped improve contrast for imaging, however the images are not satisfactory.

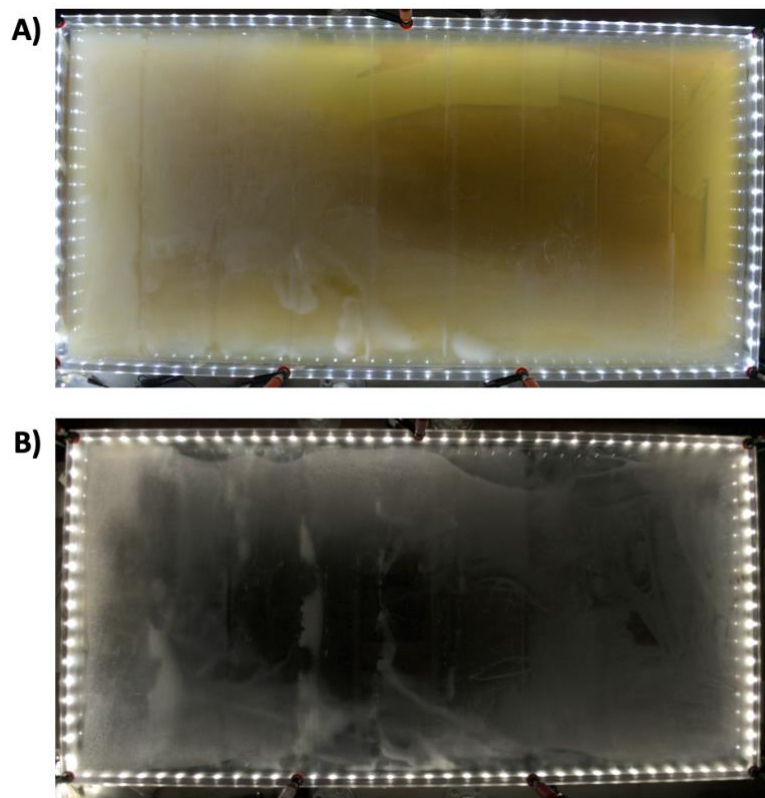


Figure 13: Effectiveness of India Ink negative staining to improve bacteria visualization on a MEGA-plate experiment. A) A snapshot of a STR-gradient MEGA-plate experiment with ISO sensitivity = 5000, without negative staining. B) A snapshot of a similar STR-

gradient MEGA-plate experiment with ISO sensitivity = 1000, including negative staining. This image was edited on Preview to maximize contrast between the bacteria and background agar.

Comparing the MEGA-plate and its prototype, it appears that the larger plate runs do not show bacterial stalling and acquisition of STR-resistance to the same resolution as seen on the miniature version. It is important to note that the MEGA-plate experiments have an additional layer of solid agar below the swim agar compared to its mini counterpart. The additional layer of solid agar functions to level off the first layer of solid agar and prevents the bacteria from interacting with the built-in partitions on the MEGA-plate. The mini-MEGA-plate does not require this layer of solid agar since temporary partitions are used to pour each slab. To evaluate the effect of a second layer of agar on STR diffusion, I repeated the STR-gradient experiments on the mini-MEGA-plate, similar to Figure 3, with and without a second layer of agar. *Salmonella* on the plates without an additional layer of agar were able to spread across the plate faster, suggesting that these bacteria likely encounter less STR due to the increased distance over which the antibiotic must diffuse to reach the swim agar.

2.8 Optimizing the MEGA-plate experimental protocol

While the MEGA-plate experiments used to investigate the evolution of antibiotic resistance in the Baym *et al.* (2016) paper included a second layer of agar, it appeared to notably affect the resolution of our STR-gradient experiment. Instead of pouring a 3 L second agar layer overlay, I covered the exposed built-in partitions with approximately 150 mL of 1% LB using a serological pipette (Fig. 14a). With the STR-agar in direct

contact with the swim agar, the antibiotic should be able to diffuse more freely. Ensuring the built-in partitions are not exposed to the swim agar will prevent bacteria from interacting and swimming along them (Fig. 14b). In the modified MEGA-plate experiment, bacteria stalled at the 100 $\mu\text{g}/\text{mL}$ STR barrier and appeared to spread across the plate more slowly compared to previous runs. However, bacteria were still able to swim into the highest concentration of STR. In addition, one of the eight built-in partitions was not adequately covered, resulting in bacteria interacting and swimming along the partition.

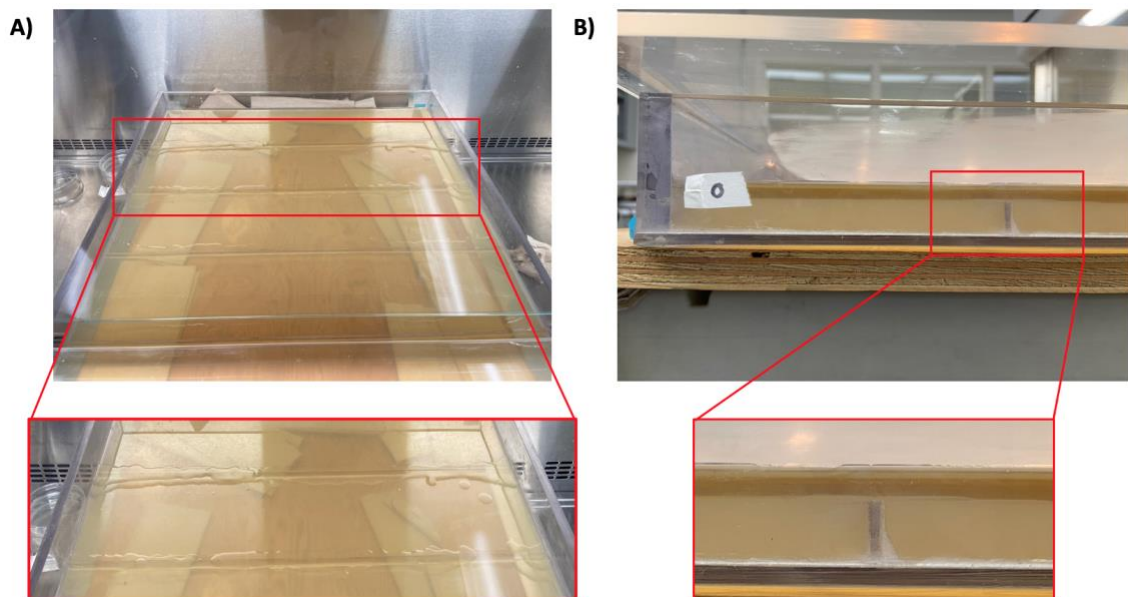


Figure 14: Minimizing the effects of the second agar layer on STR diffusion. A) A STR-gradient MEGA-plate experiment with a reduced second layer of 1% LB agar, limited to covering exposed built-in partitions. B) The modified experimental design allows the STR-LB agar to be in direct contact with the swim agar, while covering the partitions.

Across several MEGA-plate experiments, I noticed that the bacteria consistently spread towards and along the top edge of the plate despite being inoculated in the middle of a slab. This is likely due to a pooling of liquid along the top edge that appears after a few days of incubation (Fig. 15a). When the bacteria reach the liquid, it can easily spread along the edge. I suspected that the pooling of liquid was a result of uneven heating in the warm room. There is a fan that blows hot air directly above the top edge of the MEGA-plate, corresponding to the left side of the plates in Figure 15. I used bags to create a barrier to reduce the uneven heating by preventing hot air from blowing directly over the plate (Fig. 15b). This barrier reduced a considerable amount of liquid along the top edge. To further minimize the effects of uneven heating, I fortified the barrier with another layer of plastic and ensured it spans the full length of the table. I also reversed the orientation the plate during the pouring and imaging process (ie. I poured 1% LB agar without STR into the slab that I previously assigned as the highest STR-LB agar slab). By changing the orientation of the MEGA-plate and analysing whether there is decreased pooling of water, I can narrow down whether the source of liquid accumulation is the warm room or the plate itself. When the MEGA-plate was reoriented and incubated with a reinforced plastic barrier, liquid accumulated along the edge farther from the fan which is the same edge shown in Figure 15a. As such, the liquid accumulation is likely related to the plate itself.

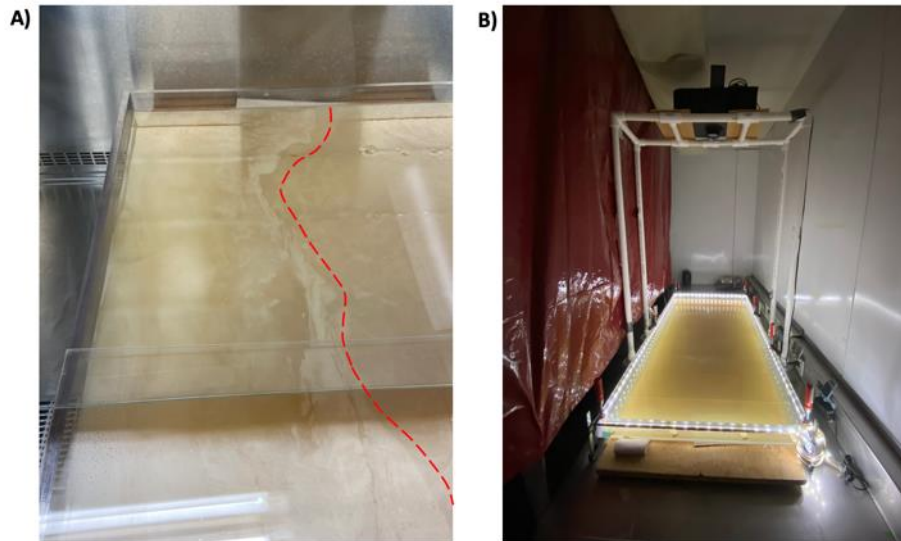


Figure 15: Accumulation of liquid on the agar interferes with the MEGA-plate experiment. A) The side of the MEGA-plate exposed to additional heat resulted in a pooling of liquid along that edge as outlined by the red dashed line. B) Red, plastic biohazard bags are used as a barrier to reduce uneven heating from a ceiling fan on the left side of the image.

2.9 Final MEGA-plate protocol with annotations

In preparation for a MEGA-plate experiment, ensure the following have been completed:

- a) The plate has been cleaned thoroughly with the most recent cleaning protocol.
- b) The plate is completely dry, paying close attention to the edges and corners of the plate. If the plate is not completely dry, the agar will mix with residual bleach, Power Quat and/or ethanol which may interfere with the experiment. If there is remaining liquid in the plate, allow it to air dry in the BSC under UV light.

c) There are enough media bottles and magnetic stir bars for 12 L of 1% LB agar and 3 L of 0.28% LB swim agar. Since each section of the first layer has a volume of 1 L, it will be easier to use a total of nine 1 L bottles and four 2 L bottles or flasks for the remaining agar. It is also advisable to make an extra bottle of 1% and 0.28% agar in case of spillage and evaporation during the autoclave run.

d) Post-autoclave, combine the agar such that nine bottles have 1 L of 1% agar, two bottles have 1.5 L of 1% agar, and two bottles have 1.5 L of 0.28% swim agar. As the agar begins to cool down, bottles should be placed in the 55°C CO₂ incubator or on a stir-plate to prevent the agar from solidifying.

When all preparations have been completed (plate is cleaned and dried, and media has been prepared), the following experimental protocol should be used:

1) Transfer the MEGA-plate with its lid onto the utility cart and slide the shorter end of the plate into the BSC. The MEGA-plate should be pushed as far into the BSC as possible but remain on the utility cart. The plate must stay on the utility cart for the duration of agar pouring for easy manipulation and to keep the plate as level as possible.

2) Use a leveler to ensure the sections of the MEGA-plate that are inside the BSC are level. Since the whole MEGA-plate is not completely flat, it is important to focus on leveling the MEGA-plate one section at a time. Putting paper towel under the plate can help raise the plate where needed.

3) Three sections of the first agar layer will be poured together. Slide the lid off the plate until the three sections of the MEGA-plate that are inside the BSC are exposed. All areas of the plate outside the BSC should be covered with the lid. Add the appropriate

stimulus to each bottle and pour as much of the 1 L agar into the assigned section as possible. Pouring the agar slowly will minimize the appearance of bubbles. Be mindful that the magnetic stir bar does not fall into the MEGA-plate. Pour the remaining agar from each bottle into empty petri dishes as control plates. Allow these three sections to completely solidify without moving the plate.

4) When the agar has solidified, slide the lid back onto the whole MEGA-plate and maneuver the utility cart and plate such that the three empty sections on the opposite end of the plate are in the BSC. Similar to Step 2, use a leveler to ensure the section of the plate inside the BSC is flat.

5) The three sections positioned in the BSC will be poured together. Add the appropriate stimulus to each 1 L bottle and follow Step 3 instructions.

6) Since the full MEGA-plate does not fit inside the BSC, it needs to be poured partially in the BSC and partially around flames. While the three outer sections on both ends of the plate can be poured inside the BSC, the middle three sections need to be poured around flames. When the previously poured agar has solidified, slide the lid back onto the whole MEGA-plate and set up three alcohol lamps along one long edge of the plate that is not in the BSC. This time, slide the lid approximately 1 inch away from edge with the alcohol lamps.

7) Add the appropriate stimulus into the remaining first layer agar bottles and pour them gently to reduce bubbles. Bubbles should burst on their own as the agar dries. Allow the agar to dry completely before moving on to Step 8.

8) Prior to pouring the second layer of agar, reconfirm the plate is leveled. For the second layer, combine a total of 3 L of 1% LB agar into two separate bottles. This layer begins to solidify within a minute of pouring so care must be taken to pour quickly, without introducing too many bubbles. Keeping the same alcohol lamp and lid configuration, pour one bottle of agar from inside the BSC and the other by the lamps through the 1-inch gap between lid and plate. Since this layer is relatively thin and solidifies quickly, it can be difficult to ensure the agar spreads evenly across the plate. As such, it is helpful to ask a fellow lab member to help with this step.

9) Once the second layer of agar has solidified, pour the swim agar as instructed in Step 8. This layer will not solidify as quickly so extra care should be taken to avoid bubbles which can interfere with imaging. This layer should be given at least 1 h to completely set. To confirm whether the swim agar has solidified, knock on the sides of the MEGA-plate or gently shake the plate.

10) To inoculate the experiment, add 100 μL of culture in four overlapping 25 μL spots. When a larger inoculum is spotted, the culture can spread across the slab as it dries especially if the plate is slightly slanted. Overlapping inoculums can be used to avoid this. The culture should be given at least 30 minutes to dry in the BSC before the lid is replaced.

11) To prepare the MEGA-plate for incubation in the warm room, a total of seven bar clamps are used to secure the lid to the plate. Four clamps are used for the corners and the remaining three are used to secure the long edges of the plate. Then, the plate is

wrapped in parafilm. The purpose of the bar clamps and parafilm is to prevent the lid from warping and the agar from drying out during incubation.

12) Tape the LED strip to the outside walls of the MEGA-plate and orient the lights to shine inwards. The LED strip should be positioned halfway between the top of the agar and the top of the plate. These LED strips act as a light source for time-series imaging and prevent the need for overhead lights, which previously produced a large glare on the lid and interfered with imaging.

13) Using the utility cart, transport the MEGA-plate to the table in the warm room. This step must be done with another lab member.

14) To capture time-series imaging, place the overhead imaging set-up as depicted in Figure 12b. Ensure all auto camera settings are adjusted to manual. If settings are left on auto, images will likely vary in terms of focus and lighting.

2.10 Future directions: Refine the experimental protocol

Based on the results of the most recent MEGA-plate run, there are several aspects of the protocol that need to be further explored and adjusted. One challenge has been the accumulation of liquid on top of the agar. In several MEGA-plate experiments, this liquid pooled along the walls, carried the bacteria down the plate and caused the bacteria to spread either from top to bottom or bottom to top, as opposed to laterally from left to right. I originally suspected this was a result of uneven heating in warm room, however water seems to accumulate along the same wall of the MEGA-plate regardless of its orientation during incubation. This suggests that there may be something inherent to the plate or experimental design that is contributing to this condensation, although several

factors may be at play. Before pouring agar into the MEGA-plate, I use a leveler to ensure each section is as flat as possible, often adjusting the position of the plate throughout the whole process since the floor and utility cart that hold the plate are not completely level. It also seems that the plate itself is lower in the middle portions (ie. the three middle sections) and often tilts toward one side, which may explain why the liquid always accumulates along the same wall. While I think it is unlikely that this unevenness is solely causing the condensation, ensuring the plate is completely flat will avoid introducing additional variables that can interfere with the experiment. This can be accomplished by pouring the plate on a flat surface like a benchtop and replacing the wooden base support with something that is resistant to warping (ex. a thicker sheet of plywood). If water continues to pool on the agar surface, it may also be worth exploring if the heating is more uniform on the other end of the warm room, away from the fan blowing hot air. If unsuccessful, it will be important to explore alternatives for incubation outside of the current warm room. Since *Salmonella* swims faster at warmer temperatures (previously compared migration rates at 37°C versus room temperature), we can incubate the plate in a small room with infrared heating panels, as suggested by Dr. Surette.

The lid is another area of improvement. In the most recent MEGA-plate run where negative staining was used, the black background agar unintentionally highlighted streak marks on the lid which were likely caused when cleaning with ethanol. Since both the bacteria and cleaning marks appear white, it becomes difficult to differentiate the two, therefore decreasing the image quality. This haze was likely present in previous experiments but less visible due to the yellow-coloured agar. Ethanol seems to leave

behind a white haze on surfaces. This can be resolved by using methanol to clean the top and underside of the lid. Alternatively, I suspect the best way to ensure maximum clarity during imaging is to use a sheet of glass as a lid. So long as the plate is evenly heated or heated from the top, condensation droplets should not be an issue.

I am currently working with Bert Visheau to construct an autoclavable MEGA-plate. While the optimized cleaning and experimental protocols have greatly reduced the amount of unwanted growth, they require a considerable amount of time and effort, and the results are inconsistent. After consulting information data sheets and a plastics expert, I chose to experiment with polyetherimide (PEI), a thermoplastic that can withstand repeated autoclaving (Devasahayam et al. 2002). Bert Visheau successfully bonded the samples of the plastic to itself and I confirmed the durability of the PEI and bonding through multiple rounds of autoclaving. We have ordered a 0.375 inch sheet of PEI to construct an autoclavable MEGA-plate that fits in the BSC (estimating 16 inch width by 48 inch length). To sterilize the plate, I intend to wrap it in aluminum foil and use the large autoclave in the Michael Degroote Centre for Learning and Discovery (MDCL). I have reached out to the MDCL autoclave room staff and will continue to coordinate with them. We will likely need to set-up or reactivate an account with them and discuss best handling practices with the MEGA-plate. Post-autoclave, I can remove the aluminum foil and pour the plate in its entirety in the BSC while maintaining sterility. This will also allow me to pour the plate on a level surface. An autoclavable MEGA-plate would make this experiment more time efficient and reduce the chances of contamination. If we are successful in building this plate, the cleaning protocol can be updated accordingly.

CHAPTER 3: ANTICIPATORY REGULATION TRAINING WITH ALTERNATING CARBON SOURCES

3.1 Learning via physical and non-landscape exposure

Adaptive laboratory evolution can be studied using physical and non-physical landscapes. On a physical landscape like the MEGA-plate, stimuli are spatially organized in an alternating manner. These stimuli are predominantly stationary and contained within their respective sections while motile bacteria swim through the predefine landscape. This approach is advantageous because variants that arise and can swim faster will be visually and spatially separated on the plate. This allows us to easily sample of variants of interest and track evolution overtime. For example, a two-step mutation can be visually identified on the plate as highlighted on Figure 3 but less evident in a broth culture. However this approach is limited because evolution is not always led by the variant that is best adapted due to spatially restrictions. Baym *et al.* (2016) discovered that some variants that were more resistant to antibiotics were trapped behind other lineages. This suggests that the fitness of the population on a plate depends partially on that the fastest swimmers may not be the most well-adapted. In addition, the agar near the partitions will likely contain both stimuli due to diffusion. Bacteria will experience temporary co-exposures to both stimuli which may affect learning. Finally, it is important to note that the visible swimming behaviours we will see on plates represent population migration as opposed to individual cells' swimming speeds. Bacterial populations can migrate more quickly than others for reasons that do not involve differences in individual swimming speeds, such as greater

sensitivity to chemotactic substances. As such, we define migration rate as how fast a bacterial population or swimming front moves across the plates.

A non-physical landscape such as serially passaging cultures in test tubes, is the most common method of studying adaptive prediction (Mitchell et al. 2009; Schild et al. 2007; Eoh et al. 2017; Adams and Rosenzweig 2014). Unlike a physical landscape, a stimulus can be completely removed in broth prior to encountering the next stimulus to ensure sequential exposure and avoid co-administration. There is also more flexibility to explore a variety of stimuli since these can easily be added or removed. However, as mentioned previously, variants of interest can be hard to isolate in broth compared to on plates since it will take many passages before those mutants start to dominate. It is likely that only the fittest mutants will persist while less-fit mutants go undetected, despite the fact that these variants can provide important mechanistic information. Stepwise mutations will also be harder to detect in broth than on plate. Furthermore, broth passaging in test tubes involves relatively smaller volumes of bacteria which may impose some evolutionary restraints. Each approach has its advantages and limitations so I experimented with conditioning on both physical and non-physical landscapes.

3.2 Conditioning with citrate and maltose

Sequential exposure to different carbon sources naturally occurs in the gut, such as the predictable switch from lactose to maltose (Savageau 1998). In an attempt to create a novel landscape, we selected two unrelated secondary carbon sources, citrate and maltose, to pilot our conditioning experiments. While citrate utilization uses the tripartite-tricarboxylate transporter (Winnen, Hvorup, and Saier 2003), maltose uptake involves an

outer membrane porin-like protein (LamB) (Schülein and Benz 1990). *Salmonella* that learn to use citrate to anticipate maltose and produce the necessary maltose metabolism proteins will be more fit, will rapidly deplete the second carbon source, and can be selected over time.

To evaluate whether *Salmonella* demonstrates asymmetrical anticipation with the citrate-maltose pairing, it is important to revisit the criteria established by Mitchell *et al.* (2009). First, the stimuli association should be unidirectional, meaning pre-exposure to citrate should generate a fitness advantage under maltose but not vice versa. While both stimuli are independently neutral, the switch from citrate to maltose as the sole carbon source creates a temporary cellular state of carbon starvation. Maltose can be viewed as a better carbon source compared to citrate as it has more carbons and is metabolized into glucose, the preferred carbon source (Kenyon et al. 2005). *Salmonella* has also been reported to grow to a higher OD with maltose as a sole carbon source compared to citrate (Kenyon et al. 2005). As such, bacteria may be more likely to form an association that anticipates a larger reward than a smaller one. In theory, it would also be more beneficial to anticipate an event that requires more time and effort during preparation than something that can be prepared quickly. For example, maltose metabolism relies on numerous proteins for uptake into the cell, including the trimeric LamB, a periplasmic maltose-binding protein, and a four-subunit inner membrane transporter, as well as additional enzymes involved in glycolysis and the Krebs cycle (Boos and Shuman 1998). On the other hand, citrate has a three-subunit transporter and only requires Krebs cycle enzymes (Rosa et al. 2018). Since maltose metabolism requires more steps and

components, it can be argued that anticipating maltose will be more beneficial than citrate. Second, preparatory behaviour for maltose should be costly to ensure that anticipation is conserved to reap a future reward that outweighs the preparatory costs. Since maltose metabolism requires the expression of different uptake and metabolic proteins, preparation in the absence of maltose will be costly. In addition, *Salmonella* that constitutively express both carbon source utilization systems will be less fit and outcompeted over time. Lastly, the association with maltose should be specific to citrate as opposed to other unrelated stimuli. All these criteria will need to be verified through experimentation to confirm the presence of asymmetrical anticipation.

3.3 Materials and Methods

3.3.1 Bacterial strains and growth conditions

For training experiments involving carbon sources, *S. Typhimurium* was grown in M9 minimal media broth (Difco™ M9 Minimal Salts, 5X [disodium phosphate anhydrous, monopotassium phosphate, sodium chloride, ammonium chloride], Becton, Dickinson and Company, Sparks, USA, Cat. # 248510) supplemented with limiting carbon (Chapter 3.5) and 10 mM MgSO₄, which was necessary for growth. Cultures were supplemented with citrate (Sodium citrate tribasic dihydrate, Sigma-Aldrich, St. Louis, USA, Cat. # C8532-500), maltose (D-(+)-Maltose monohydrate, Sigma-Aldrich, St. Louis, USA, Cat. #M5885-500) or D-glucose (Dextrose anhydrous, Fisher Chemical, Fair Lawn, USA, Cat. #D16-1).

3.3.2 Citrate-maltose training in broth

S. Typhimurium LT2 was grown overnight from a frozen stock or previously passaged cultured in 10 mL of M9 minimal media broth supplemented with limiting 7.81 mM glucose and 10 mM MgSO₄. The culture was transferred to a Falcon™ 15 mL conical centrifuge tube, pelleted via centrifugation at 7000 g for 5 min, and washed once with 5 mL M9 minimal media broth. The washed pellet was resuspended in 10 mL of M9 minimal media broth supplemented with 7.81 mM citrate and 10 mM MgSO₄, and incubated at 130 RPM at 37°C for 15 minutes. These cells were pelleted via centrifugation at 7000 g for 5 min, and washed once with 5 mL M9 minimal media broth. The washed pellet was resuspended in 450 µL of M9 minimal media broth and inoculated into several test tubes of 10 mL of M9 minimal media broth supplemented with 0.98 mM limiting maltose and 10 mM MgSO₄. For passages 1-4, 100 µL of resuspended cells was inoculated resulting in initial ODs ranging from 0.07 to 0.15. With subsequent passages, I intentionally inoculated with smaller volumes to reach the targeted initial optical density (OD) reading of 0.050 and doubled the limiting maltose concentration to 1.95 mM. This allows me to increase the number of generations *Salmonella* is exposed to maltose during training by two and standardize the experiment. The cultures were incubated overnight at 130 RPM at 37°C and OD measurements were taken. The overnight cultures were transferred to 50 mL conical centrifuge tubes, pelleted via centrifugation at 7000 g for 5 min, and washed once with 5 mL M9 minimal media broth. The washed pellet was resuspended in 800 µL of M9 minimal media broth and 850 µL of the resuspension was transferred to a frozen stock tube containing 150 µL of glycerol.

3.3.3 Citrate-maltose training on the mini-MEGA-plate

The mini-MEGA-plates used for the carbon source training experiments were performed using Nunc™ OmniTray™ Single-Well Plates. The plates are divided into four equal sections along the long edge of the plate, each section's area measuring 2.9 x 7.5 cm. These measurements are marked on the bottom of the plates and used as guides when using temporary partitions for pouring different media conditions. Initially, disposable pipetting reservoirs were used as temporary partitions required for pouring sections of different media conditions. These reservoirs were cut to size (7.5 cm length) using ethanol-sterilized scissors, soaked in an ethanol bath for appropriate 20 minutes, and air dried in the BSC. In later iterations of these training experiments, autoclavable partitions made from PEI, cut by Bert Visheau, were used as the temporary partitions to minimize risks of contamination. These partitions are autoclaved once a week for sterilization and further sterilized with ethanol between experiments within a week. For each section, 5 mL of 1% M9 minimal media agar supplemented with 10 mM MgSO₄ and 50 µg/mL Kanamycin (KAN) (Kanamycin sulfate, Fisher BioReagents, Fair Lawn, USA, Cat. # BP9065) is aliquoted into a test tube and the appropriate amount of citrate or maltose is added. The test tubes are vortexed gently and contents of the tubes are poured into the appropriate section of the OmniTray plate. Once the agar has set, the temporary partition is removed and placed at the next section's measurement marking. A total of four sections are poured, with alternating citrate and maltose in adjacent sections. Approximately 25-30 mL of 0.28% M9 minimal media swim agar supplemented with 10 mM MgSO₄ and 50 µg/mL KAN is overlaid, ensuring that the first layer of agar is

completely covered. A 2 μL inoculum of an overnight bacterial culture grown in limiting 7.81 mM glucose supplemented with 10 mM MgSO_4 is spotted 1 cm from the edge of the plate (equidistance from the top and bottom edge) on the leftmost section containing citrate. The plates are secured with parafilm and incubated at 37°C in the Epson Perfection V850 Pro Scanner. A bash script is used to capture time series images every 30 minutes for the duration of the experiment through the Raspberry Pi 3 (B+ Model) (adapted from French, Coutts, and Brown 2018). The images are compiled in iMovie to create time series imaging.

When the bacterial swimming front has crossed into the last maltose section or reached the end of the plate, a serological pipette is used to sample the swim agar of the entire swimming front. The sample is centrifuged at 7000 g for 5 minutes to spin down bacterial cells. The supernatant is discarded, and the pellet and soft agar are resuspended in 5 mL M9 broth. The resuspension is centrifuged at 7000 g for 5 minutes and the supernatant is discarded. The pellet is resuspended in approximately 500 μL of M9 minimal media broth. 850 μL of the resuspension is transferred to two frozen stock tubes containing 150 μL of glycerol.

3.4 Training on a physical landscape with the mini-MEGA-plate

To piloting the citrate-maltose pairing on a physical landscape, I used the mini-MEGA-plate. These plates consist of alternating M9 minimal media agar slabs supplemented with either citrate or maltose as the sole carbon source. I poured a layer of low percentage (0.28%) swim agar over top and inoculated 2 μL of overnight culture of *S. Typhimurium* LT2 grown in M9 media with limiting (7.81 mM) glucose on the leftmost

slab containing citrate. I supplemented both agar layers with 50 $\mu\text{g/mL}$ KAN to suppress contamination. I also supplemented all M9 media and agar with 10 mM MgSO_4 which was necessary to promote bacterial growth. To record time-series imaging, I used a flatbed scanner to image the plates every 30 minutes. When the bacterial swimming front passed into the rightmost slab containing maltose, I sampled the front to select for the fastest swimming bacteria, “the winners”, and created a frozen stock. Subsequent passaging of *S. Typhimurium* LT2 through alternating citrate and maltose using the mini-MEGA-plate will be inoculated with an overnight culture of “the winners” from the previous experiment.

Figure 16a depicts time series imaging of the first passage of *S. Typhimurium* LT2 through the citrate-maltose pairing on the mini-MEGA-plate. Both carbon sources were supplemented at 31.25 mM, an optimized concentration resulting in an ideal migration rate that allows me to sample the bacterial swimming front before it reaches the end of the plate. As the bacteria encounter alternating carbon sources, there is evidence of reduced motility seen as a flattening of the swimming front (T=19 h, 27 h, 32 h) and variants capable of swimming faster through maltose (T=32 h). The colored, dashed lines represent different swimming fronts tracked through imaging. During the first passage, there appears to be three swimming fronts: a faster, fainter front (blue), a slower, more prominent front (red), and the slowest, faint front (green). The fastest, faint swimming front might be a result of swarmer cells, however additional analysis is required for confirmation. I stopped the experiment after 36 hours of incubation when the more prominent (red) front passed into the rightmost slab and sampled the front.

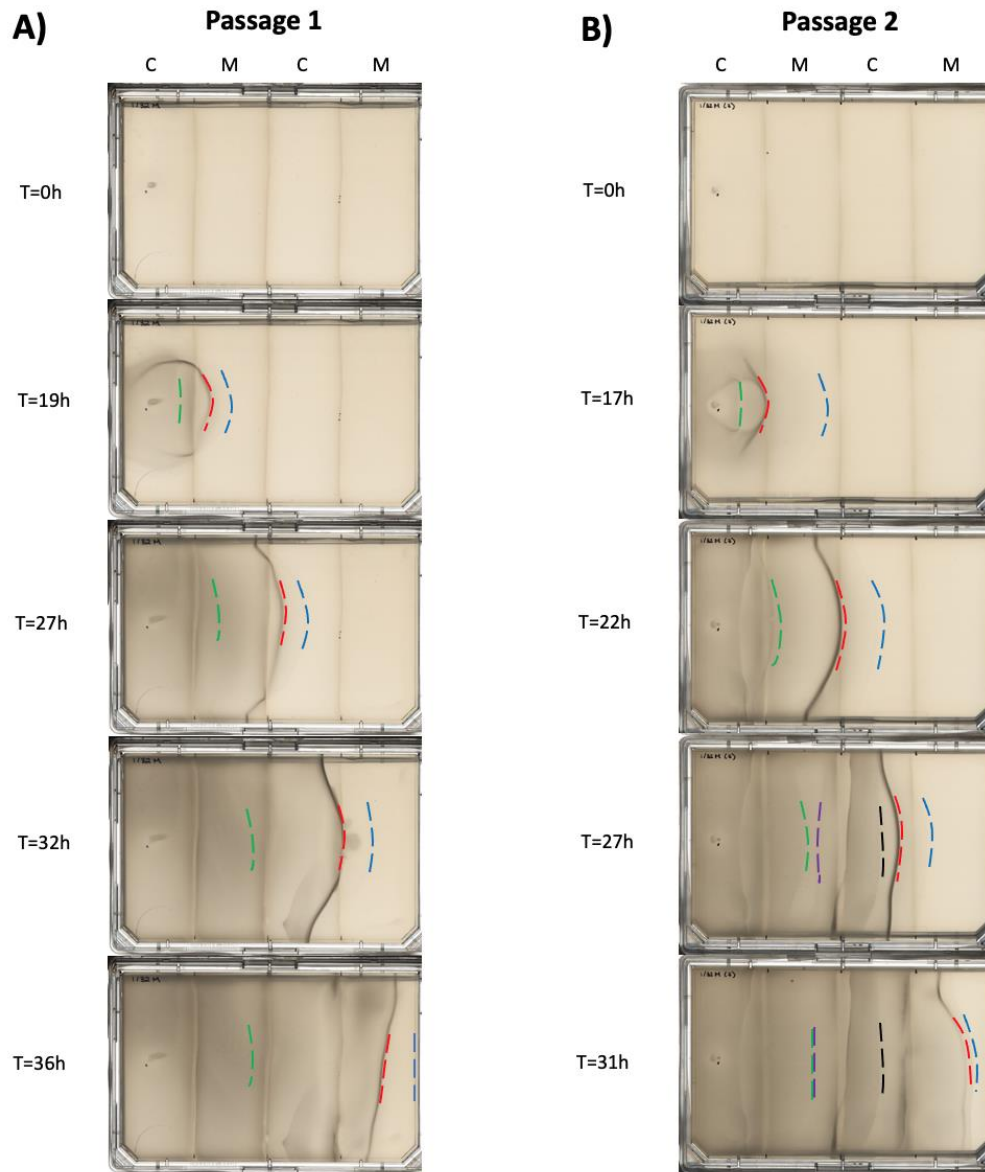


Figure 16: Time series imaging of *S. Typhimurium* LT2 passages through the citrate-maltose stimuli pairing on a mini-MEGA-plate. a) Passage one and b) two time series imaging highlighted at select timepoints. Slabs were supplemented with either 31.25 mM citrate (C) or maltose (M). The colored, dashed lines correspond to different swimming fronts that can be tracked over different time points. The time points were selected to best illustrate a) reduced motility at each partition and the appearance of a variant in the first

passage, and b) the appearance and movement of different swimming fronts in the second passage.

Time series imaging of the second passage of *S. Typhimurium* LT2 through the citrate-maltose pairing shows more complexity and is illustrated by Figure 16b. An overnight culture of “the winners” from passage 1 was grown in M9 minimal media with limiting glucose and used to inoculate the second passage. Four technical replicates were imaged and showed similar swimming patterns, hence only one replicate is shown. Three visible swimming fronts corresponding to the blue, red, and green dashed lines can be tracked as they move across the plate. At T=27 h, there appears to be a new swimming front (purple) in the second slab that moves in the opposite direction toward the left side of the plate. It is possible that this front represents a portion of bacteria that 1) cannot turn on its citrate metabolism genes quick enough to take advantage of the new carbon source and must turn back around to consume the remaining maltose, or 2) chooses to swim back towards maltose since it is the preferred carbon source over citrate. In both cases, the mini-MEGA-plate approach correctly selects against this subpopulation of bacteria that 1) may be slower to adapt to an environmental change, or 2) does not swim the length of the MEGA-plate which prevents it from encountering repetitions of the citrate-maltose pairing. Theoretically after multiple passages, despite the environmental shift, bacteria that have acquired anticipatory regulation can sense citrate and anticipate an abundance of maltose. The second citrate slab also appears to have bacteria that gets left behind as shown by the black line (T=27 h, 31 h). This may have resulted from the exhaustion of a carbon source or nutrient or the presence of a chemorepellent. Bacteria in the second

mini-MEGA-plate passage swam across the plate faster than the first passage, needing only 31 hours of incubation to reach the rightmost slab, however differences between inoculum sizes and batches of swim agar may contribute to this observation. As such for future passages, I standardized the inoculum size and included a control, a mini-MEGA-plate with alternating citrate-maltose slabs that is inoculated with a naïve *S. Typhimurium* LT2 culture that has not undergone passaging. This allowed me to compare the migration rate of passaged bacteria relative to naïve bacteria.

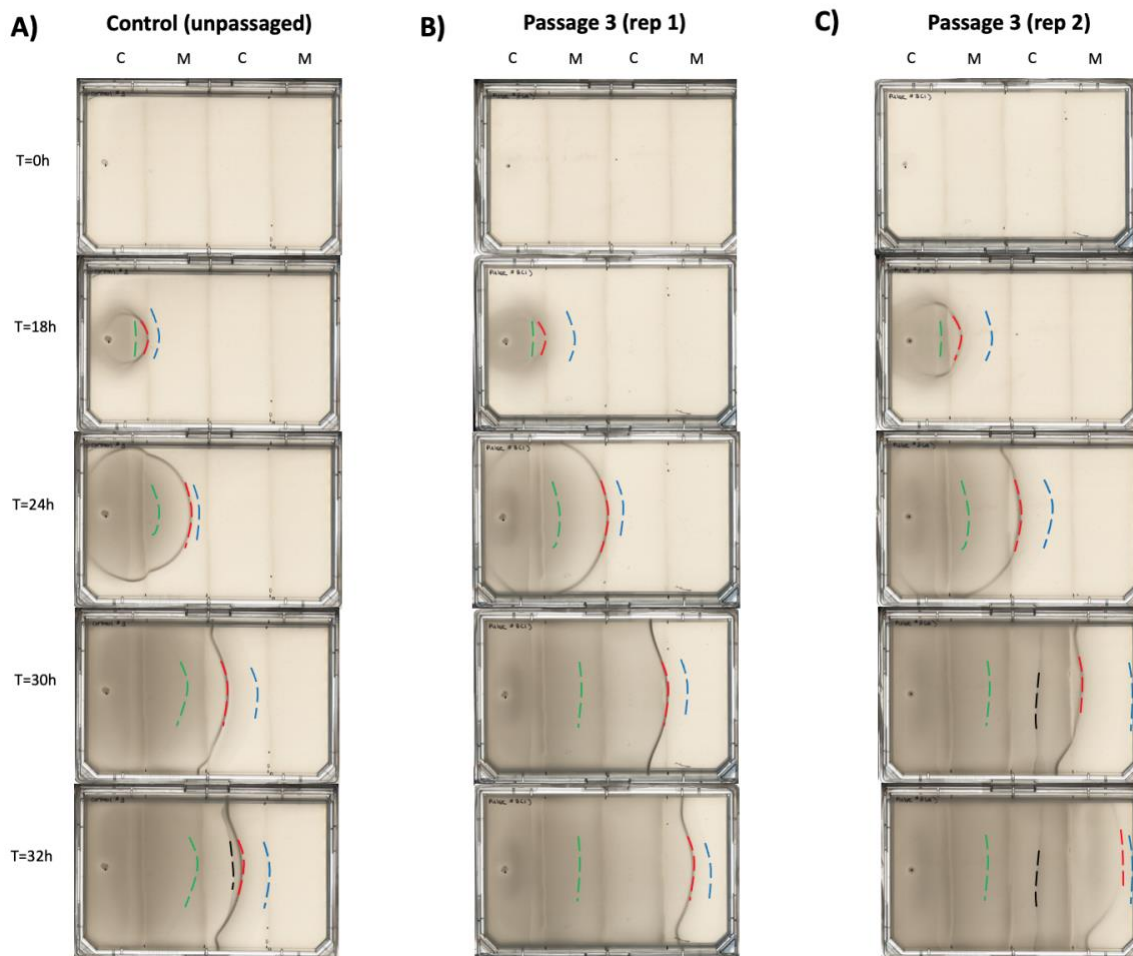


Figure 17: Time series imaging of *S. Typhimurium* LT2 passage three through the citrate-maltose stimuli pairing using a mini-MEGA-plate prototype. Slabs were

supplemented with either 31.25 mM citrate (C) or maltose (M). The colored, dashed lines correspond to different swimming fronts that can be tracked over different time points.

The time points were selected to best illustrate differences in swimming behaviours and migration rates between naïve (a) and passaged cells (b, c) and within technical replicates.

Time series imaging of *S. Typhimurium* LT2 undergoing a third passage alongside naïve cells is depicted in Figure 17. Separate overnight cultures of “the winners” from passage 2 and naïve cells from the original parent freezer stock were grown in M9 minimal media with limiting glucose to a standardized OD of 0.9. I plated three technical replicates of the passage three mini-MEGA-plates and imaging showed two distinct swimming patterns (Fig. 17b and 17c). Comparing within technical replicates, there are three initial swimming fronts (blue, red, green dashed lines) that can be tracked across all the plates which is similar to previous passages. However, only two of the three technical replicates displayed a phenotype that resembles bacteria being left behind, represented by the black dashed line. This phenotype is also seen on the control plate (Fig. 17a) and passage two plates (Fig. 16b). When comparing passage two and three bacterial swimming behaviours, the third passage plates do not show any evidence of bacteria swimming back toward the left side of the plate. Most importantly, passaged *S. Typhimurium* LT2 swim through the mini-MEGA-plate landscape notably faster than naïve *S. Typhimurium* LT2 in as little as two passages or four citrate-maltose exposures. To calculate how fast the passaged cells were migrating relative to the control, I measured the distance from the front of the inoculum spot to the furthest point on the blue and red propagating fronts that continued to advance. At T=32 h, the blue swimming front on

passage three replicate one (Fig. 16b) and replicate two (Fig. 16c) migrated 1.3X and 1.4X faster than the control. The red swimming front on passage three replicates migrated 1.4X and 1.6X faster than the control. The mini-MEGA-plate conditioning experiments appear to have selected for faster swimmers, although there was only one instance on passage one where a visible mutant arose.

3.5 Determining limiting concentration ranges of carbon sources

For the training experiments, it is important to standardize the initial inoculum so experiments can be comparable. For overnight cultures of *S. Typhimurium*, I wanted to use a limiting concentration of glucose that would prevent the culture from entering stationary phase and accumulating toxin. At the same time, I wanted to ensure that the stalled OD would be relatively high so I could start my training experiment with a large number of cells. Figure 18 depicts several growth curves of *S. Typhimurium* LT2 grown in M9 minimal media supplemented with MgSO₄ and a range of glucose (15.62 – 0 mM). From these growth curves, I chose to use limiting 7.81 mM glucose for overnight cultures as this concentration begins to stall at a relatively high OD.

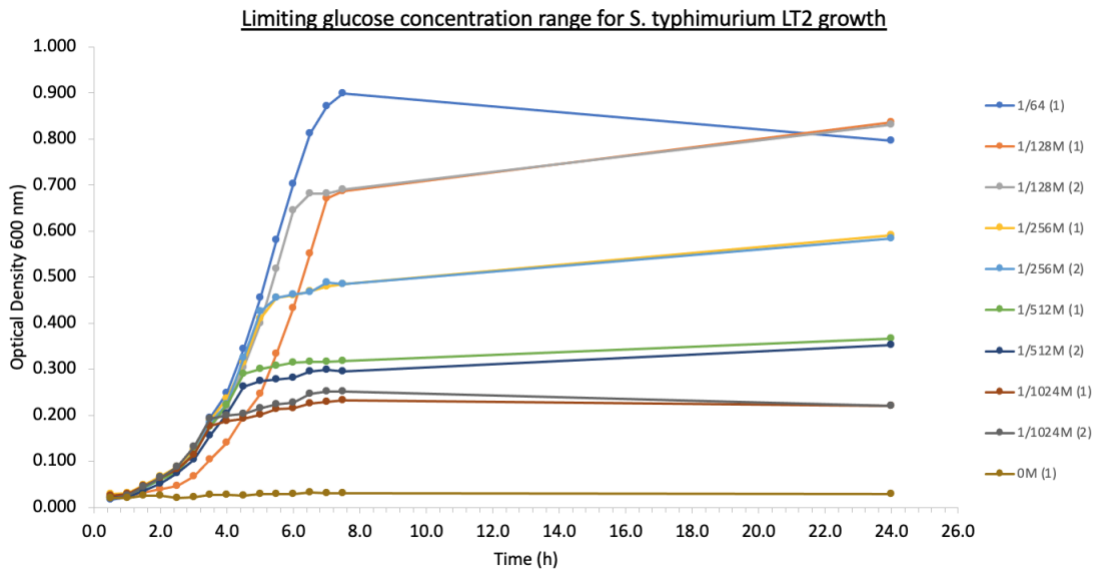


Figure 18: Determining the concentration range of limiting glucose for an overnight culture of *S. Typhimurium* LT2. Culture containing glucose concentrations 7.81 mM, 3.91 mM, 1.95 mM and 0.98 mM were tracked in duplicated while 0 mM and 15.62 mM glucose were tracked as a single replicate. Tubes were incubated at 37°C shaking at 130 RPM and removed for brief periods of time for OD (600 nm) measurements using a spectrophotometer.

The purpose of limiting maltose in the training experiment is to create additional evolutionary pressure to select for bacteria that can consume maltose faster without constitutively expressing maltose metabolism genes. To optimize the maltose concentration used on the broth training experiment, it was important to consider the timeframe of the experiment. Figure 19 depicts several growth curves of *S. Typhimurium* LT2 grown in M9 minimal media supplemented with $MgSO_4$ and a range of maltose (31.25 mM – 0.49 mM). From these growth curves, I initially chose to use limiting 0.98 mM maltose because growth stalled after approximately 11 h. This allowed me to

complete the broth training experiment within a single day and perform more passages. However from passage five onwards, I doubled the maltose concentration to 1.95 mM and incubated the cultures overnight to increase the number of generations *S. Typhimurium* LT2 spends in maltose within a single passage.

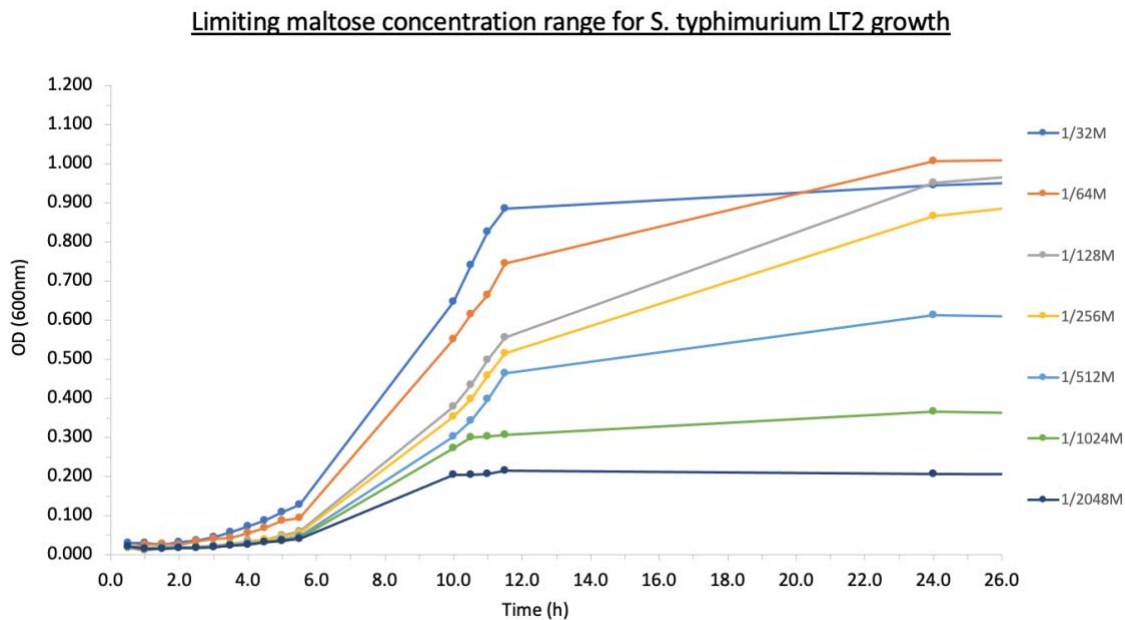


Figure 19: Determining the concentration range of limiting maltose for an overnight culture of *S. Typhimurium* LT2. Maltose concentrations from 0.49 mM to 31.25 mM were tracked as single replicates. Tubes were incubated at 37°C shaking at 130 RPM and removed for brief periods of time for OD (600 nm) measurements using a spectrophotometer.

3.6 Training with a non-physical landscape in broth

To explore citrate-maltose conditioning in a non-physical landscape, I serially passaged bacteria in broth. *S. Typhimurium* LT2 is grown in M9 minimal media with limiting glucose to a standardized optical density (OD) of 0.8-0.9. These cells are washed

with M9 media to remove excess glucose and incubated in M9 media supplemented with 7.81 mM citrate and 10 mM MgSO₄ for 15 minutes. A short incubation time in citrate was chosen to allow the cells to sense but not metabolize the carbon source.

Consequently, transcriptional activation of citrate metabolism genes is not beneficial. The cells are washed with M9 media to remove excess citrate and grown in several M9 media tubes supplemented with limiting maltose which creates additional pressure to select for bacteria that can consume maltose faster. These tubes are concentrated into a single frozen stock, passaged back through limiting glucose to counter-select against constitutive mutants favoring maltose metabolism, and used to inoculate the subsequent passaging experiment. This experimental design aims to select for bacteria that turn on maltose metabolism genes in the presence of citrate, but in anticipation of an upcoming maltose environment. Tracking the duration of the lag phase can indicate how well the bacteria are metabolizing the carbon source, with shorter lag phases suggesting faster or anticipatory utilization. Figure 20 depicts a growth curve of *S. Typhimurium* LT2 during the second maltose passage in broth with a lag phase of approximately 7.5 h. To determine the lag phase, a line was extrapolated along the steepest slope of the log phase which represents the fastest growth rate. Another line is extended from the initial OD of the culture. The x-coordinate of the intersection between these two lines indicates the duration of the lag phase. To determine when stationary phase is reached, a horizontal line is drawn across the maximum culture OD. The x-coordinate of the intersection between the slope line and maximum OD line indicates the start of stationary, which is approximately 11.5 h.

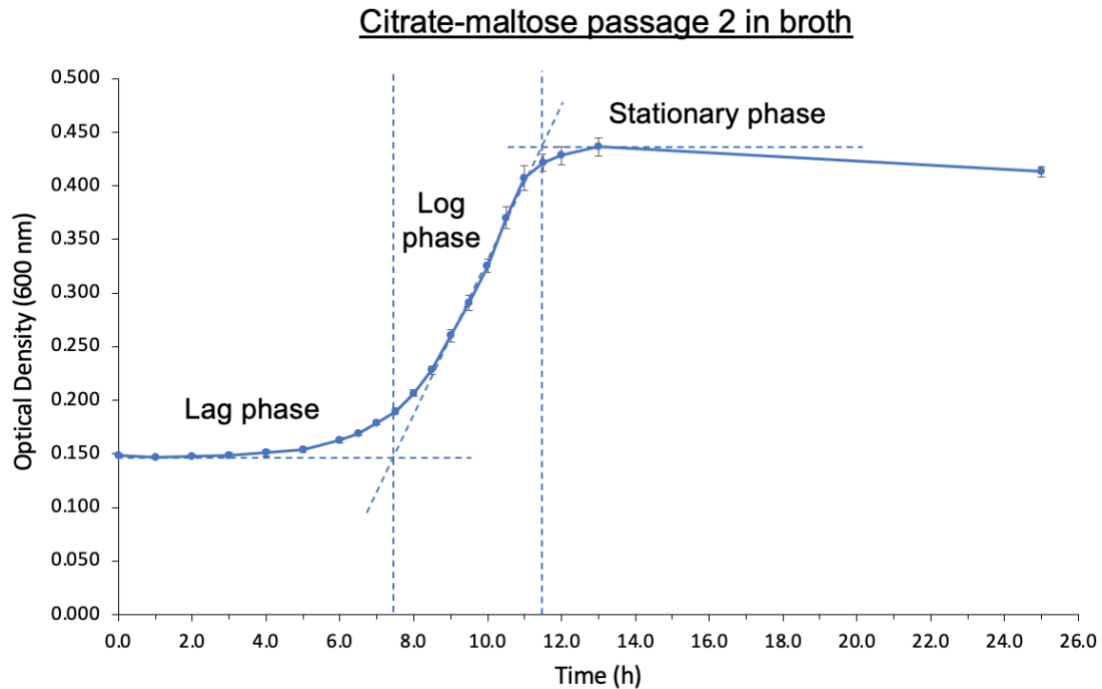


Figure 20: *S. Typhimurium* LT2 growth curve in M9 media with limiting maltose during citrate-maltose broth passage. Data points represent the mean of six technical replicates of cultures from the second broth passage with standard deviation error bars. The blue dashed lines are used to graphically determination the lag, log and stationary phase of the growth curve.

To date, I have passaged *S. Typhimurium* LT2 through the citrate-maltose pairing 11 times in broth, totalling approximately 30 generations. For passages one to four (initial OD ranging from 0.07 to 0.15; limiting 0.98 mM maltose), OD was measured in 30-minute intervals. While this allowed me to track the growth curves of individual passages, it would be difficult to compare these curves across passages since initial OD was not standardized. In addition, this method of tracking growth curves for each passage was also incredibly time consuming. For subsequent passages (initial OD standardized to 0.05,

limiting 1.96 mM maltose), I simply recorded the initial and final OD to calculate the number of generations. Since the cells of each passage will be stocked, I can return to specific passages and track their growth curves in a single day.

3.7 Summary of training results

To pilot conditioning on a physical landscape, I standardized a training experiment on the mini-MEGA-plate with alternating sections of citrate and maltose. On the first passage, there was evidence of two emerging variants that arose at the second citrate-maltose barrier which were able to swim faster through maltose (Fig. 16a). Since the cells from this lineage previously encountered another citrate-maltose transition, it is possible that some bacteria retained molecular or cellular products that allowed these cells to swim faster through maltose. It may be possible that some cells have already created an association between these carbon sources and are demonstrating anticipatory regulation, however this is highly unlikely to occur after a single encounter. Instead, it is more likely that we have selected for cells that are faster swimmers. This phenotype is advantageous as it allows the cells to be the first to explore an upcoming nutrient-rich environment. It is important to distinguish that the fastest swimmers may not necessarily be the best adapted or have acquired anticipatory regulation. As such, additional genetic and transcriptional analyses using techniques such as genome sequencing, RNA-seq and gene reporter constructs are needed.

In all passages on the mini-MEGA-plate, there are three initial swimming fronts (blue, red, green) that can be tracked across the plate. This pattern of chemotactic rings forms due to cells aggregating towards a gradient of chemoattractant amino acids that the

bacteria produce themselves (Woodward et al. 1995). It is also possible that the first swimming front is created by swarmer cells since the low population density, interpreted from the faintness of the front, is unlikely to generate a strong enough gradient for chemotaxis demonstrated by the second, more dominant front. Microscope analysis of cells at different swimming fronts can confirm whether there are swarmer cells.

Alternatively, this fainter front may be caused by a chemorepellent force generated from the second, more dominant swimming front. More complex swimming behaviours appear in passages two. When bacteria encounter the second section of citrate, a portion of the population moves in the opposite direction back toward the previous maltose section (Fig 16b, purple dashed line). It is possible that these backward-swimming bacteria either 1) turn back around to consume the remaining maltose because they have not turned on their citrate metabolism genes quickly enough to take advantage of the new carbon source, or 2) choose to swim back towards maltose since it is the preferred carbon source over citrate. In both cases, the mini-MEGA-plate approach correctly selects against this subpopulation of bacteria since after multiple passages, we hope to select bacteria that have acquired anticipatory regulation and use citrate to anticipate an upcoming abundance of maltose. At the second citrate section on plate from passage two and three, there also appears to be a portion of bacteria that gets left behind as shown by the black dashed lines (Fig 16b, Fig 17c). Since this phenotype appears after bacteria have already moved across this area, this may be a result of nutrient exhaustion or the accumulation of a chemorepellent released from *Salmonella*. Different swimming behaviours may suggest differences in how maltose and citrate are being metabolized by the winners and losers.

Analyzing the contents and chemotactic effects of supernatants from various passages may provide insight into potential metabolic changes and anticipatory mechanisms at play.

Most notably, I demonstrated that passaged *S. Typhimurium* LT2 swims through the mini-MEGA-plate landscape faster than naïve *S. Typhimurium* LT2 in as little as two passages or four citrate-maltose exposures. For future analyses and passaging, it will be helpful to quantify migration rates by creating a manual method or code to track swimming distance relative to time.

To pilot conditioning on a non-physical landscape, I have standardized a training experiment in broth with alternating pulses of citrate and maltose. Same day growth curve comparisons of different passages can be performed when *S. Typhimurium* has been exposed to citrate-maltose training for a sufficient number of generations, for example 50 (López García de Lomana et al. 2017). In future passages, it would be beneficial to maximize the number of training generations within a single passage. This can be achieved by using a constitutive luciferase mutant which allows low OD cultures to be measured accurately. Alternatively, cultures can be grown over a longer period of time in higher concentrations of maltose. The serial passaging approach can also be upscaled to larger volumes in flasks or the chemostat which would allow for longer exposure to maltose and prevent the culture from reaching stationary phase. Serial passaging in tubes may eventually select for mutants that do not enter stationary phase, resulting in a shorter lag phase. Further analysis into the effects of stationary phase on *Salmonella* and related adaptations should be investigated.

CHAPTER 4: CONCLUSIONS AND FUTURE DIRECTIONS

Pavlovian conditioning, or training new behaviours through anticipation, has been studied almost exclusively in eukaryotes. The little work that has been conducted on prokaryotes focuses on naturally existing examples of behavioural anticipation. This thesis aims to explore conditioning through the active training of new behaviours in *Salmonella* using a unique MEGA-plate approach.

To date, a considerable amount of optimization has been conducted to create standardized cleaning, imaging and experimental MEGA-plate protocols. While much progress has been made with the cleaning protocol, contamination is likely to continue being an obstacle. Additional adjustments need to be made to the imaging and experimental protocols, particularly to increase image quality and resolve the liquid accumulation. While there are still several aspects that need to be modified, the advantages that a physical landscape approach brings anticipatory behavioural training is compelling. As seen on the STR-gradient and citrate-maltose mini-MEGA-plate experiments, training bacteria on a physical landscape allows for easy visualization, tracking and sampling of lineages that arise that cannot be replicated in a liquid culture. While the mini-MEGA-plate experiments have demonstrated promising results, these prototypes are relatively small and contribute stricter spatial constraints. As such, training on the mini-MEGA-plate will likely require many passages to evolve variants that have learned to use citrate to anticipate maltose. By upscaling to the larger MEGA-plate, a wider propagation front will increase the mutational supply to accelerate evolution and larger distances between stimuli will help increase selection among adjacent lineages

(Baym et al. 2016). To take advantage of this unique approach while optimizing the aforementioned protocols, we plan to build and use a slightly smaller autoclavable MEGA-plate for the upscaled citrate-maltose training experiments.

If we are successful manipulating bacterial behaviour through training, this approach uncovers new avenues for therapeutics and microbiology research. By studying bacterial conditioning and the factors involved, we can further understand how bacteria evolve and exploit memory to problem solve. In addition, as we learn how to manipulate bacterial behaviour, there is an opportunity to generate populations of bacteria that are primed to anticipate select environments and are therefore more sensitive. For example, a probiotic can be trained *in vitro* where two stimuli are repeatedly paired. When these cells are administered to a patient, the bacteria are already anticipating the stimulus pairing and will be more sensitive. Finally, there are applications in therapy where reprogramming bacteria at the level of functionality may be more effective than altering community composition.

REFERENCES

- Acar, Murat, Jerome T. Mettetal, and Alexander van Oudenaarden. 2008. “Stochastic switching as a survival strategy in fluctuating environments.” *Nature Genetics* 40 (4): 471–75. <https://doi.org/10.1038/ng.110>.
- Adams, Julian, and Frank Rosenzweig. 2014. “Experimental microbial evolution: History and conceptual underpinnings.” *Genomics* 104 (6 Pt A): 393–98. <https://doi.org/10.1016/j.ygeno.2014.10.004>.
- Adler, J. 1966. “Chemotaxis in bacteria.” *Science (New York, N.Y.)* 153 (3737): 708–16. <https://doi.org/10.1126/science.153.3737.708>.
- Altier, Craig. 2005. “Genetic and environmental control of *Salmonella* invasion.” *Journal of Microbiology (Seoul, Korea)* 43 Spec No (February): 85–92.
- Balaban, Nathalie Q., Jack Merrin, Remy Chait, Lukasz Kowalik, and Stanislas Leibler. 2004. “Bacterial persistence as a phenotypic switch.” *Science* 305 (5690): 1622–25. <https://doi.org/10.1126/science.1099390>.
- Barrangou, Rodolphe, Christophe Fremaux, H el ene Deveau, Melissa Richards, Patrick Boyaval, Sylvain Moineau, Dennis A. Romero, and Philippe Horvath. 2007. “CRISPR provides acquired resistance against viruses in prokaryotes.” *Science* 315 (5819): 1709–12. <https://doi.org/10.1126/science.1138140>.
- Bauer, F. F., and I. S. Pretorius. 2000. “Yeast stress response and fermentation efficiency: How to survive the making of wine - A Review.” *South African Journal of Enology and Viticulture* 21 (1): 27–51. <https://doi.org/10.21548/21-1-3557>.

- Baumbach, Jens, Henrike Hoeke, Friderike Weege, Arne Gunnar Schmeisky, and Petra Neumann-Staubitz. 2012. “*Salmonella enterica* modulates its infectivity in response to intestinal stimuli.” *Open Journal of Medical Microbiology* 2 (2): 41–45. <https://doi.org/10.4236/ojmm.2012.22006>.
- Baym, Michael, Tami D. Lieberman, Eric D. Kelsic, Remy Chait, Rotem Gross, Idan Yelin, and Roy Kishony. 2016. “Spatiotemporal microbial evolution on antibiotic landscapes.” *Science* 353 (6304): 1147–51. <https://doi.org/10.1126/science.aag0822>.
- Beckwith, Jonathan R. 1967. “Regulation of the *lac* operon.” *Science* 156 (3775): 597–604.
- Bentley, Ronald, and E. Haslam. 1990. “The shikimate pathway — A metabolic tree with many branches.” *Critical Reviews in Biochemistry and Molecular Biology* 25 (5): 307–84. <https://doi.org/10.3109/10409239009090615>.
- Berg, Howard C., and Douglas A. Brown. 1972. “Chemotaxis in *Escherichia coli* analysed by three-dimensional tracking.” *Nature* 239 (5374): 500–504. <https://doi.org/10.1038/239500a0>.
- Bjarnason, Jaime, Carolyn M. Southward, and Michael G. Surette. 2003. “Genomic profiling of iron-responsive genes in *Salmonella enterica* serovar Typhimurium by high-throughput screening of a random promoter library.” *Journal of Bacteriology* 185 (16): 4973–82. <https://doi.org/10.1128/JB.185.16.4973-4982.2003>.
- Boos, Winfried, and Howard Shuman. 1998. “Maltose/maltodextrin system of

Escherichia coli: Transport, metabolism, and regulation.” *Microbiology and Molecular Biology Reviews* 62 (1): 204–29.

<https://doi.org/10.1128/MMBR.62.1.204-229.1998>.

Boyer, Sébastien, Lucas Hérisant, and Gavin Sherlock. 2021. “Adaptation is influenced by the complexity of environmental change during evolution in a dynamic environment.” *PLOS Genetics* 17 (1): e1009314.

<https://doi.org/10.1371/journal.pgen.1009314>.

Dekel, Erez, and Uri Alon. 2005. “Optimality and evolutionary tuning of the expression level of a protein.” *Nature* 436 (7050): 588–92.

<https://doi.org/10.1038/nature03842>.

Devasahayam, Sheila, David J. T. Hill, Peter J. Pomery, and Andrew K. Whittaker. 2002. “The radiation chemistry of Ultem at 77K as revealed by ESR spectroscopy.”

Radiation Physics and Chemistry 64 (4): 299–308. [https://doi.org/10.1016/S0969-806X\(01\)00498-4](https://doi.org/10.1016/S0969-806X(01)00498-4).

Edwards, Jessica C., Mark S. Johnson, and Barry L. Taylor. 2006. “Differentiation between electron transport sensing and proton motive force sensing by the Aer and Tsr receptors for aerotaxis.” *Molecular Microbiology* 62 (3): 823–37.

<https://doi.org/10.1111/j.1365-2958.2006.05411.x>.

Eoh, Hyungjin, Zhe Wang, Emilie Layre, Poonam Rath, Roxanne Morris, D. Branch Moody, and Kyu Y. Rhee. 2017. “Metabolic anticipation in *Mycobacterium tuberculosis*.” *Nature Microbiology* 2 (8): 1–7.

<https://doi.org/10.1038/nmicrobiol.2017.84>.

- Fernando, Chrisantha T, Anthony M.L Liekens, Lewis E.H Bingle, Christian Beck, Thorsten Lenser, Dov J Stekel, and Jonathan E Rowe. 2009. “Molecular circuits for associative learning in single-celled organisms.” *Journal of The Royal Society Interface* 6 (34): 463–69. <https://doi.org/10.1098/rsif.2008.0344>.
- French, Shawn, Brittney E. Coutts, and Eric D. Brown. 2018. “Open-source high-throughput phenomics of bacterial promoter-reporter strains.” *Cell Systems* 7 (3): 339-346.e3. <https://doi.org/10.1016/j.cels.2018.07.004>.
- Frye, Jonathan, Joyce E. Karlinsey, Heather R. Felise, Bruz Marzolf, Naeem Dowidar, Michael McClelland, and Kelly T. Hughes. 2006. “Identification of new flagellar genes of *Salmonella enterica* serovar Typhimurium.” *Journal of Bacteriology* 188 (6): 2233–43. <https://doi.org/10.1128/JB.188.6.2233-2243.2006>.
- Gal-Mor, Ohad, Erin C. Boyle, and Guntram A. Grassl. 2014. “Same species, different diseases: How and why typhoidal and non-typhoidal *Salmonella enterica* serovars differ.” *Frontiers in Microbiology* 5 (August): 391. <https://doi.org/10.3389/fmicb.2014.00391>.
- Garneau, Josiane E., Marie-Ève Dupuis, Manuela Villion, Dennis A. Romero, Rodolphe Barrangou, Patrick Boyaval, Christophe Fremaux, Philippe Horvath, Alfonso H. Magadán, and Sylvain Moineau. 2010. “The CRISPR/Cas bacterial immune system cleaves bacteriophage and plasmid DNA.” *Nature* 468 (7320): 67–71. <https://doi.org/10.1038/nature09523>.
- Harshey, R M, and T Matsuyama. 1994. “Dimorphic transition in *Escherichia coli* and *Salmonella* Typhimurium: Surface-induced differentiation into hyperflagellate

swarmer cells.” *Proceedings of the National Academy of Sciences of the United States of America* 91 (18): 8631–35.

Harvey, P. C., M. Watson, S. Hulme, M. A. Jones, M. Lovell, A. Berchieri, J. Young, N. Bumstead, and P. Barrow. 2011. “*Salmonella enterica* serovar Typhimurium colonizing the lumen of the chicken intestine grows slowly and upregulates a unique set of virulence and metabolism genes ∇ .” *Infection and Immunity* 79 (10): 4105–21. <https://doi.org/10.1128/IAI.01390-10>.

Hazelbauer, G. L. 1975. “Maltose chemoreceptor of *Escherichia coli*.” *Journal of Bacteriology* 122 (1): 206–14. <https://doi.org/10.1128/jb.122.1.206-214.1975>.

Hoffmann, Stefanie, Christiane Schmidt, Steffi Walter, Jennifer K. Bender, and Roman G. Gerlach. 2017. “Scarless deletion of up to seven methyl-accepting chemotaxis genes with an optimized method highlights key function of CheM in *Salmonella* Typhimurium.” *PLOS ONE* 12 (2): e0172630. <https://doi.org/10.1371/journal.pone.0172630>.

Jones, B. D., N. Ghori, and S. Falkow. 1994. “*Salmonella* Typhimurium initiates murine infection by penetrating and destroying the specialized epithelial M cells of the Peyer’s patches.” *The Journal of Experimental Medicine* 180 (1): 15–23. <https://doi.org/10.1084/jem.180.1.15>.

Kenyon, William J., Sheena M. Thomas, Erin Johnson, Mark J. Pallen, and Michael P. Spector. 2005. “Shifts from glucose to certain secondary carbon-sources result in activation of the extracytoplasmic function sigma factor ΣE in *Salmonella*

enterica serovar Typhimurium.” *Microbiology (Reading, England)* 151 (Pt 7): 2373–83. <https://doi.org/10.1099/mic.0.27649-0>.

Koirala, Santosh, Patrick Mears, Martin Sim, Ido Golding, Yann R. Chemla, Phillip D. Aldridge, and Christopher V. Rao. 2014. “A nutrient-tunable bistable switch controls motility in *Salmonella enterica* serovar Typhimurium.” *MBio* 5 (5): e01611-14. <https://doi.org/10.1128/mBio.01611-14>.

Kondoh, H, C B Ball, and J Adler. 1979. “Identification of a methyl-accepting chemotaxis protein for the ribose and galactose chemoreceptors of *Escherichia coli*.” *Proceedings of the National Academy of Sciences of the United States of America* 76 (1): 260–64.

Kortman, Guus A. M., Annemarie Boleij, Dorine W. Swinkels, and Harold Tjalsma. 2012. “Iron availability increases the pathogenic potential of *Salmonella* Typhimurium and other enteric pathogens at the intestinal epithelial interface.” *PLOS ONE* 7 (1): e29968. <https://doi.org/10.1371/journal.pone.0029968>.

Kröger, Carsten, Shane C. Dillon, Andrew D. S. Cameron, Kai Papenfort, Sathesh K. Sivasankaran, Karsten Hokamp, Yanjie Chao, et al. 2012. “The transcriptional landscape and small RNAs of *Salmonella enterica* serovar Typhimurium.” *Proceedings of the National Academy of Sciences of the United States of America* 109 (20): E1277–86. <https://doi.org/10.1073/pnas.1201061109>.

Kuranda, Klaudia, Veronique Leberre, Serguei Sokol, Grazyna Palamarczyk, and Jean François. 2006. “Investigating the caffeine effects in the yeast *Saccharomyces cerevisiae* brings new insights into the connection between TOR, PKC and

Ras/CAMP signalling pathways.” *Molecular Microbiology* 61 (5): 1147–66.

<https://doi.org/10.1111/j.1365-2958.2006.05300.x>.

Lambert, Guillaume, and Edo Kussell. 2014. “Memory and fitness optimization of bacteria under fluctuating environments.” *PLoS Genetics* 10 (9): e1004556.

<https://doi.org/10.1371/journal.pgen.1004556>.

Lazova, Milena D., Mitchell T. Butler, Thomas S. Shimizu, and Rasika M. Harshey.

2012. “*Salmonella* chemoreceptors McpB and McpC mediate a repellent response to L-cystine: A potential mechanism to avoid oxidative conditions.” *Molecular Microbiology* 84 (4): 697–711.

<https://doi.org/10.1111/j.1365-2958.2012.08051.x>.

Lee, Calvin K., Jaime de Anda, Amy E. Baker, Rachel R. Bennett, Yun Luo, Ernest Y.

Lee, Joshua A. Keefe, et al. 2018. “Multigenerational memory and adaptive adhesion in early bacterial biofilm communities.” *Proceedings of the National Academy of Sciences of the United States of America* 115 (17): 4471–76.

<https://doi.org/10.1073/pnas.1720071115>.

López García de Lomana, Adrián, Amardeep Kaur, Serdar Turkarslan, Karlyn D. Beer,

Fred D. Mast, Jennifer J. Smith, John D. Aitchison, and Nitin S. Baliga. 2017. “Adaptive prediction emerges over short evolutionary time scales.” *Genome Biology and Evolution* 9 (6): 1616–23. <https://doi.org/10.1093/gbe/evx116>.

Lou, Lixin, Peng Zhang, Rongli Piao, and Yang Wang. 2019. “*Salmonella* pathogenicity

island 1 (SPI-1) and its complex regulatory network.” *Frontiers in Cellular and Infection Microbiology* 9.

<https://www.frontiersin.org/article/10.3389/fcimb.2019.00270>.

- Macnab, R. M., and D. E. Koshland. 1972. “The gradient-sensing mechanism in bacterial chemotaxis.” *Proceedings of the National Academy of Sciences of the United States of America* 69 (9): 2509–12. <https://doi.org/10.1073/pnas.69.9.2509>.
- Mager, W. H., and S. Hohmann. 1997. “Introduction: Stress response: Mechanism in the yeast *Saccharomyces cerevisiae*.” *Yeast Stress Responses.*, 1–6.
- Majowicz, Shannon E., Jennie Musto, Elaine Scallan, Frederick J. Angulo, Martyn Kirk, Sarah J. O’Brien, Timothy F. Jones, Aamir Fazil, Robert M. Hoekstra, and International Collaboration on Enteric Disease “Burden of Illness” Studies. 2010. “The global burden of nontyphoidal *Salmonella* gastroenteritis.” *Clinical Infectious Diseases: An Official Publication of the Infectious Diseases Society of America* 50 (6): 882–89. <https://doi.org/10.1086/650733>.
- Mariconda, Susana, Qingfeng Wang, and Rasika M. Harshey. 2006. “A mechanical role for the chemotaxis system in swarming motility.” *Molecular Microbiology* 60 (6): 1590–1602. <https://doi.org/10.1111/j.1365-2958.2006.05208.x>.
- Maris, Angel F., André L.K. Assumpção, Diego Bonatto, Martin Brendel, and João Antônio P. Henriques. 2001. “Diauxic shift-induced stress resistance against hydroperoxides in *Saccharomyces cerevisiae* is not an adaptive stress response and does not depend on functional mitochondria.” *Current Genetics* 39 (3): 137–49. <https://doi.org/10.1007/s002940100194>.
- McClelland, Michael, Kenneth E. Sanderson, John Spieth, Sandra W. Clifton, Phil Latreille, Laura Courtney, Steffen Porwollik, et al. 2001. “Complete genome

sequence of *Salmonella enterica* serovar Typhimurium LT2.” *Nature* 413 (6858): 852–56. <https://doi.org/10.1038/35101614>.

Miller, S I, and J J Mekalanos. 1990. “Constitutive expression of the PhoP regulon Attenuates *Salmonella* virulence and survival within macrophages.” *Journal of Bacteriology* 172 (5): 2485–90. <https://doi.org/10.1128/jb.172.5.2485-2490.1990>.

Mitchell, Amir, Gal H. Romano, Bella Groisman, Avihu Yona, Erez Dekel, Martin Kupiec, Orna Dahan, and Yitzhak Pilpel. 2009. “Adaptive prediction of environmental changes by microorganisms.” *Nature* 460 (7252): 220–24. <https://doi.org/10.1038/nature08112>.

Mitchell, Amir, and Yitzhak Pilpel. 2011. “A mathematical model for adaptive prediction of environmental changes by microorganisms.” *Proceedings of the National Academy of Sciences* 108 (17): 7271–76. <https://doi.org/10.1073/pnas.1019754108>.

Mojica, F. J. M., C. Díez-Villaseñor, J. García-Martínez, and C. Almendros. 2009. “Short motif sequences determine the targets of the prokaryotic CRISPR defence system.” *Microbiology*, 155 (3): 733–40. <https://doi.org/10.1099/mic.0.023960-0>.

Novick, Aaron, and Milton Weiner. 1957. “Enzyme induction as an all-or-none phenomenon.” *Proceedings of the National Academy of Sciences* 43 (7): 553–66. <https://doi.org/10.1073/pnas.43.7.553>.

Ozbudak, Ertugrul M, Mukund Thattai, Han N Lim, Boris I Shraiman, and Alexander van Oudenaarden. 2004. “Multistability in the lactose utilization network of *Escherichia coli*” 427: 4.

- Patteson, A. E., A. Gopinath, M. Goulian, and P. E. Arratia. 2015. “Running and tumbling with *E. coli* in polymeric solutions.” *Scientific Reports* 5 (1): 15761. <https://doi.org/10.1038/srep15761>.
- Pavlov, I. P. 1927. *Conditioned reflexes: An investigation of the physiological activity of the cerebral cortex*. Oxford, England: Oxford Univ. Press.
- Rallis, Charalampos, Sandra Codlin, and Jürg Bähler. 2013. “TORC1 signaling inhibition by rapamycin and caffeine affect lifespan, global gene expression, and cell proliferation of fission yeast.” *Aging Cell* 12 (4): 563–73. <https://doi.org/10.1111/accel.12080>.
- Rolfe, Matthew D., Christopher J. Rice, Sacha Lucchini, Carmen Pin, Arthur Thompson, Andrew D. S. Cameron, Mark Alston, et al. 2012. “Lag phase is a distinct growth phase that prepares bacteria for exponential growth and involves transient metal accumulation.” *Journal of Bacteriology* 194 (3): 686–701. <https://doi.org/10.1128/JB.06112-11>.
- Rosa, Leonardo T., Matheus E. Bianconi, Gavin H. Thomas, and David J. Kelly. 2018. “Tripartite ATP-independent periplasmic (TRAP) transporters and tripartite tricarboxylate transporters (TTT): From uptake to pathogenicity.” *Frontiers in Cellular and Infection Microbiology* 8. <https://www.frontiersin.org/article/10.3389/fcimb.2018.00033>.
- Savageau, Michael A. 1998. “Demand theory of gene regulation. II. Quantitative application to the lactose and maltose operons of *Escherichia coli*.” *Genetics* 149 (4): 1677–91.

- Schild, Stefan, Rita Tamayo, Eric J. Nelson, Firdausi Qadri, Stephen B. Calderwood, and Andrew Camilli. 2007. “Genes induced late in infection increase fitness of *Vibrio cholerae* after release into the environment.” *Cell Host & Microbe* 2 (4): 264–77.
<https://doi.org/10.1016/j.chom.2007.09.004>.
- Schülein, K., and R. Benz. 1990. “LamB (maltoporin) of *Salmonella* Typhimurium: Isolation, purification and comparison of sugar binding with LamB of *Escherichia coli*.” *Molecular Microbiology* 4 (4): 625–32.
<https://doi.org/10.1111/j.1365-2958.1990.tb00631.x>.
- Stoebel, Daniel M., Antony M. Dean, and Daniel E. Dykhuizen. 2008. “The cost of expression of *Escherichia coli* lac operon proteins is in the process, not in the products.” *Genetics* 178 (3): 1653–60.
<https://doi.org/10.1534/genetics.107.085399>.
- Tagkopoulos, Ilias, Yir-Chung Liu, and Saeed Tavazoie. 2008. “Predictive behavior within microbial genetic networks.” *Science* 320 (5881): 1313–17.
<https://doi.org/10.1126/science.1154456>.
- Webre, Daniel J., Peter M. Wolanin, and Jeffrey B. Stock. 2003. “Bacterial chemotaxis.” *Current Biology* 13 (2): R47–49.
[https://doi.org/10.1016/S0960-9822\(02\)01424-0](https://doi.org/10.1016/S0960-9822(02)01424-0).
- Winnen, Brit, Rikki N. Hvorup, and Milton H. Saier. 2003. “The tripartite tricarboxylate transporter (TTT) family.” *Research in Microbiology* 154 (7): 457–65.
[https://doi.org/10.1016/S0923-2508\(03\)00126-8](https://doi.org/10.1016/S0923-2508(03)00126-8).
- Woodward, D E, R Tyson, M R Myerscough, J D Murray, E O Budrene, and H C Berg.

1995. “Spatio-temporal patterns generated by *Salmonella* Typhimurium.”

Biophysical Journal 68 (5): 2181–89.

Xavier, Joao B., and Kevin R. Foster. 2007. “Cooperation and conflict in microbial

biofilms.” *Proceedings of the National Academy of Sciences* 104 (3): 876–81.

<https://doi.org/10.1073/pnas.0607651104>.

Yamamoto, K, and Y Imae. 1993. “Cloning and characterization of the *Salmonella*

Typhimurium-specific chemoreceptor Tcp for taxis to citrate and from

phenol.” *Proceedings of the National Academy of Sciences of the United States of*

America 90 (1): 217–21.

Zoetendal, Erwin G., Caroline M. Plugge, Antoon D. L. Akkermans, and Willem M.

de Vos. 2003. “*Victivallis vadensis* gen. nov., sp. nov., a sugar-fermenting

anaerobe from human faeces.” *International Journal of Systematic and*

Evolutionary Microbiology 53 (1): 211–15. <https://doi.org/10.1099/ijms.0.02362-0>.

